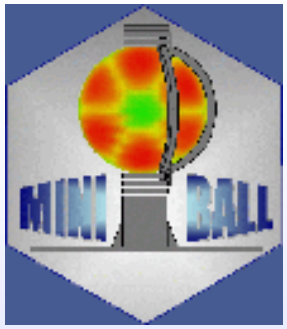

A new highly-segmented β–γ-detection set-up at LISOL

Oleg V. Ivanov, Dieter Pauwels, Maria Sawicka,
Mark Huyse, Piet Van Duppen, Yuri Kudryavtsev,
Paul Van den Bergh, Johnny Gentens,
Thomas Cocolios, Jarno Van de Walle, Andrey Andreyev

Katholieke Universiteit Leuven
Instituut voor Kern- & Stralingsfysica

Outline

1. **Introduction**
   - Experimental challenges in β-decay γ-ray spectroscopy
   - *Nuclear-structure studies at LISOL*
2. **Experimental set-up**
   - *The LISOL facility*
   - New β–γ-detection set-up
3. **β-decay of ^{65,66,67}Fe**
   - Experimental results: *spectra, half-lives, βγγ-coincidences*
   - *Discussion: the level schemes, interpretation*
4. **Conclusion and outlook**
   - Summary of performed work
   - Further nuclear-structure studies with the new set-up

See talk by Dieter Pauwels on β-decay of ^{65,66,67}Fe

Beta-decay Studies at LISOL

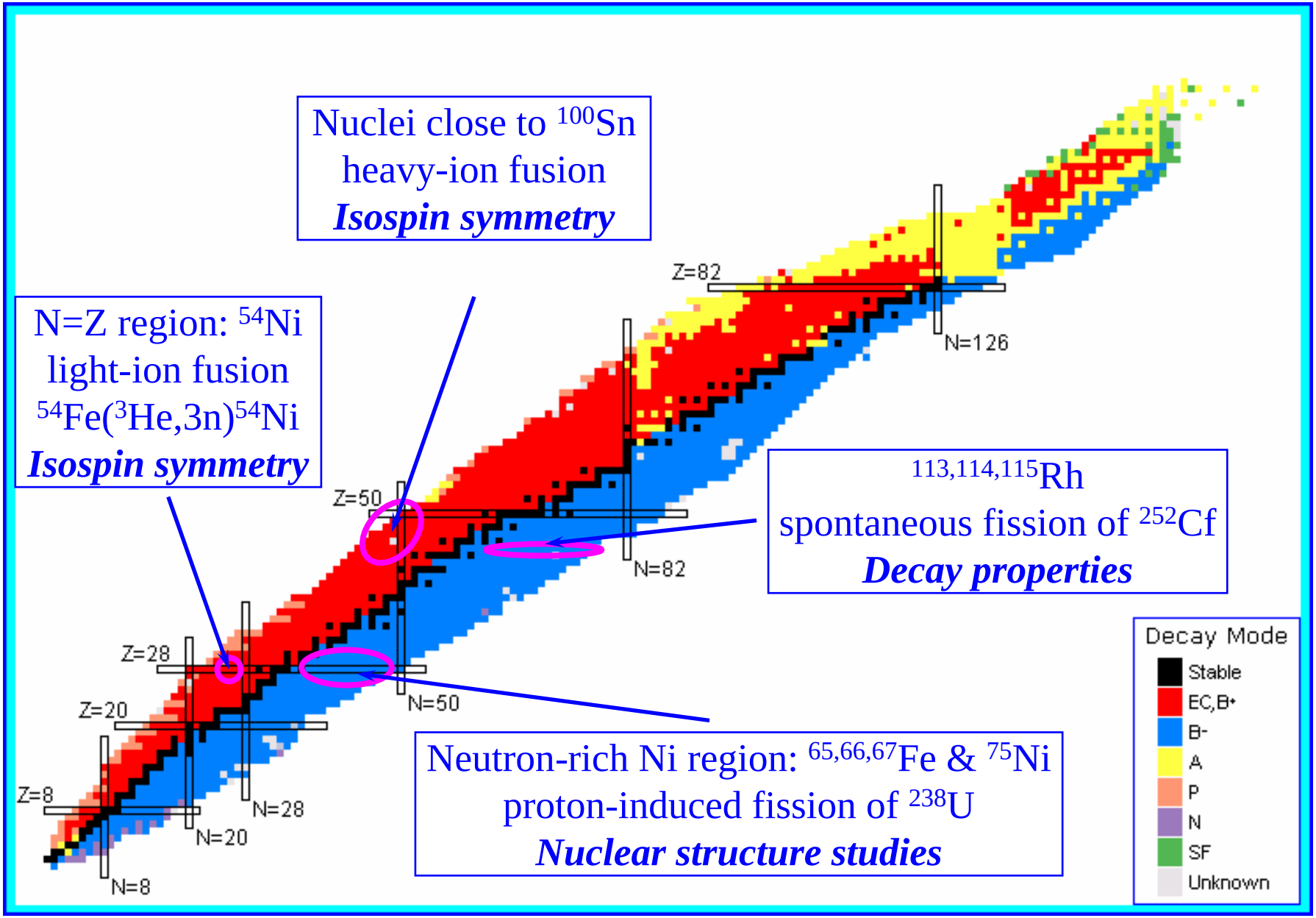

Production of neutron-rich Fe isotopes at LISOL in proton-induced fission of ^{238}U

Experimental production rates in atoms/μC for neutron-rich $^{65-69}$Fe, $^{65-70}$Co, $^{68-74}$Ni, $^{70-76}$Cu, and $^{74-81}$Ga isotopes produced at LISOL in induced fission of ^{238}U by 30 MeV protons. Except for the Fe isotopes, the values are taken from [63]. The corresponding values for the Fe isotopes are extracted by extrapolating Gaussian distribution parameters for Co, Ni, and Cu isotopes and, thus, the error bars are not provided. See text for more detail.

Atomic mass	Fe	Co	Ni	Cu	Ga
65	6.6	7 (3)			
66	4.3	10 (4)			
67	1.7	16 (5)			
68	0.4	11 (3)	16 (3)		
69	0.06	7 (3)	23 (4)		
70		1.3 (3)	28 (5)	12 (2)	
71			14 (3)	25 (7)	
72			5 (1)	65 (14)	
73			1.4 (3)	45 (10)	
74			0.20 (5)	21 (5)	5(2)
75				8 (4)	33 (8)
76				2 (1)	76 (6)
77					119 (21)
78					102 (8)
79					79 (8)
80					26 (4)
81					9(2)

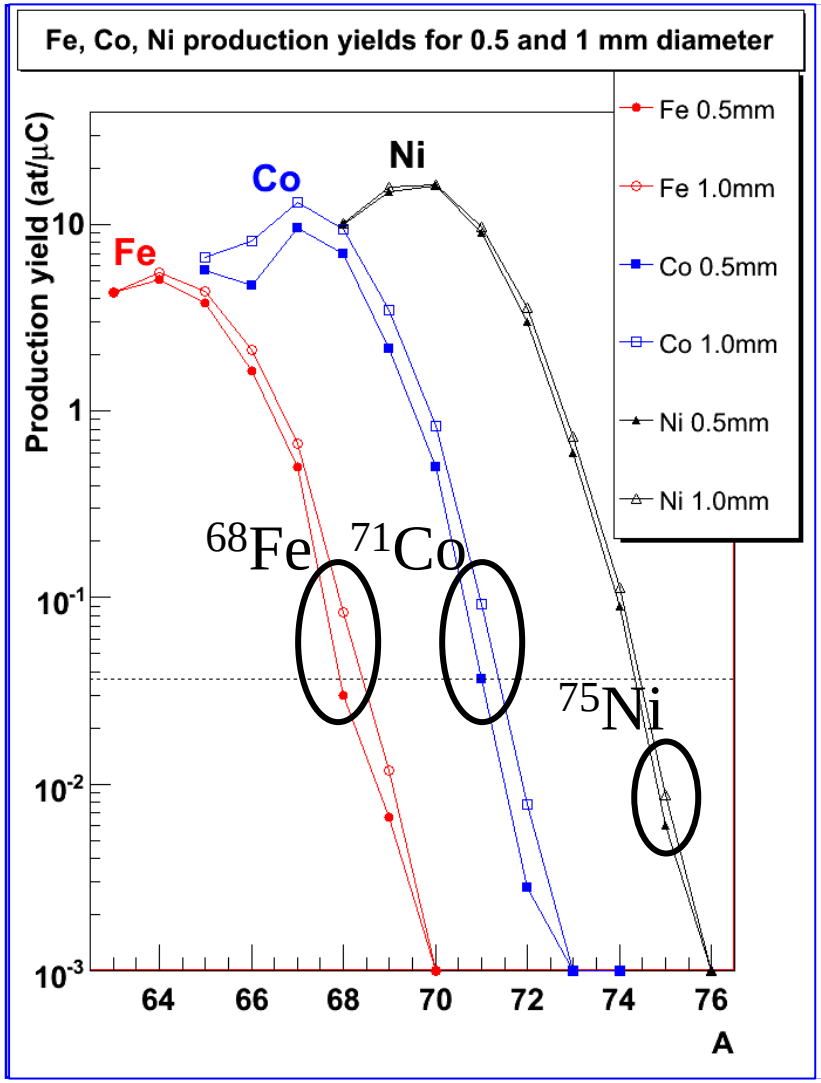

^{65,66,67}Fe are most feasible cases for the moment, ^{68}Fe is possible in the future

The main experimental challenges in γ-radiation detection

Incomplete energy absorption → Lower efficiency

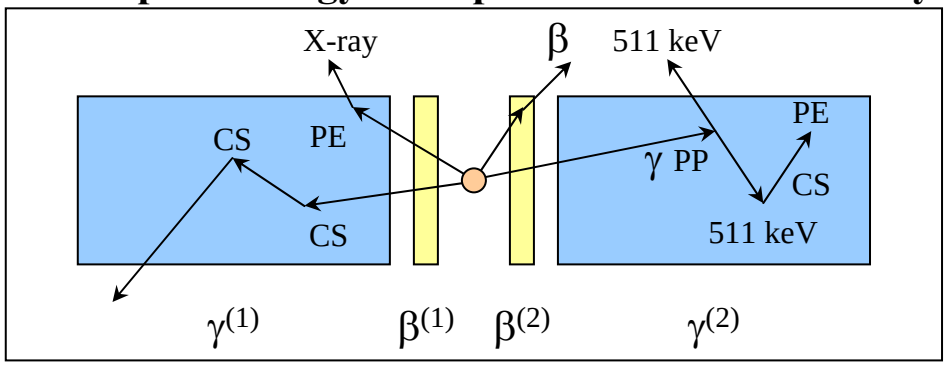

- **Compton scattering (CS) escapes**
- **Pair production (PP) annihilation escapes**
- **Photoelectric absorption X-ray escapes**

1 MeV γ-ray on standard HPGe coaxial detector:
~10% without interaction, ~70% escape,
Only ~20% are totally absorbed

Low granularity → True-coincidence summing

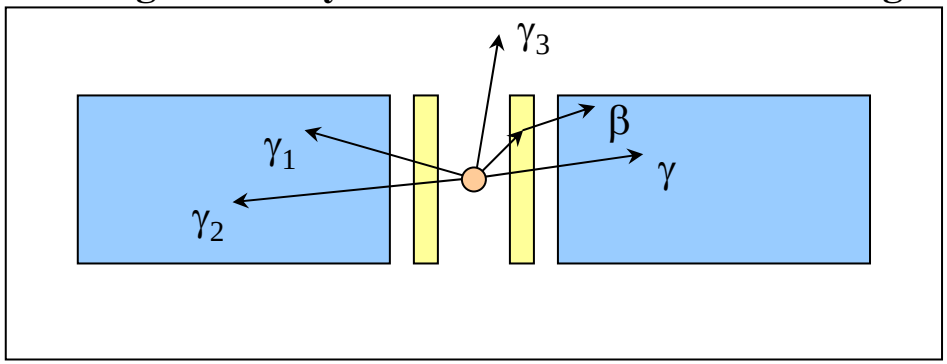

True coincidence summing of γ-rays, β-particles, Bremsstrahlung
A cascade of 1 MeV γ-rays on a standard HPGe coaxial single-crystal detector:
3 γ-rays: reduction in efficiency by ~1.2

Incomplete selectivity → Wrong coincidences

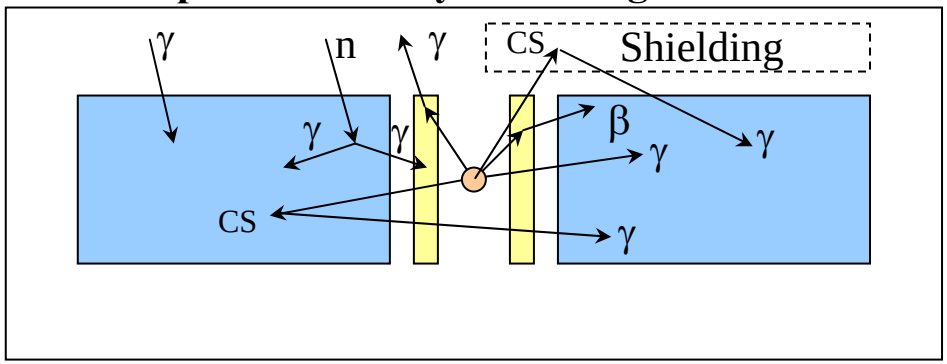

Incomplete selectivity due to sensitivity of
β-detectors to γ-radiation: ~1–2%
γ-detectors to β-particles: up to ~50%
β-, γ-detectors to cosmic radiation: up to 100%
⇒ **Wrong coincidences**

β-decay studies with highly-segmented detectors

a). Single-crystal γ-detectors

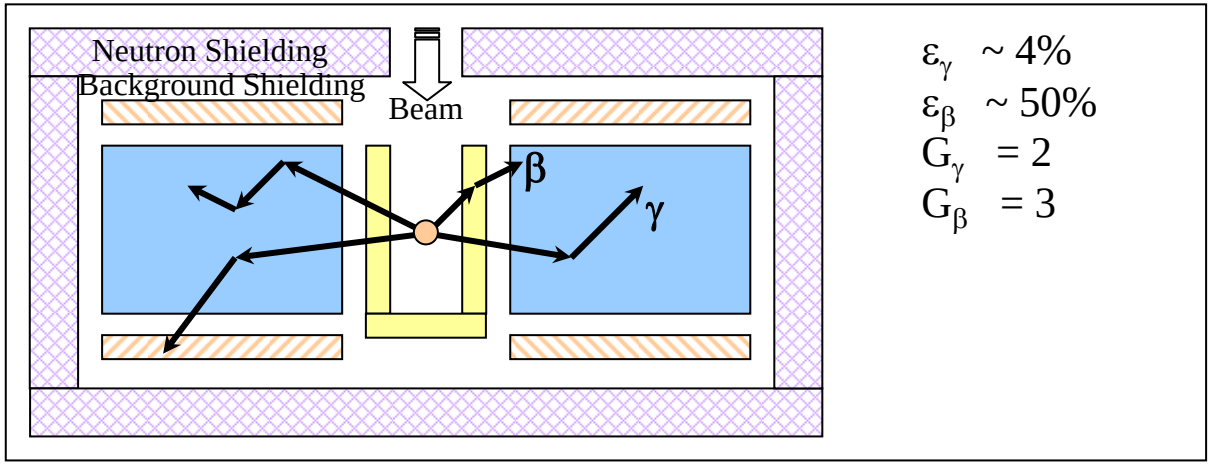

ε_γ ~ 4%
ε_β ~ 50%
G_γ = 2
G_β = 3

b). Multi-crystal γ-detectors + segmented β-detectors

c). Multi-crystal highly-segmented γ-detectors

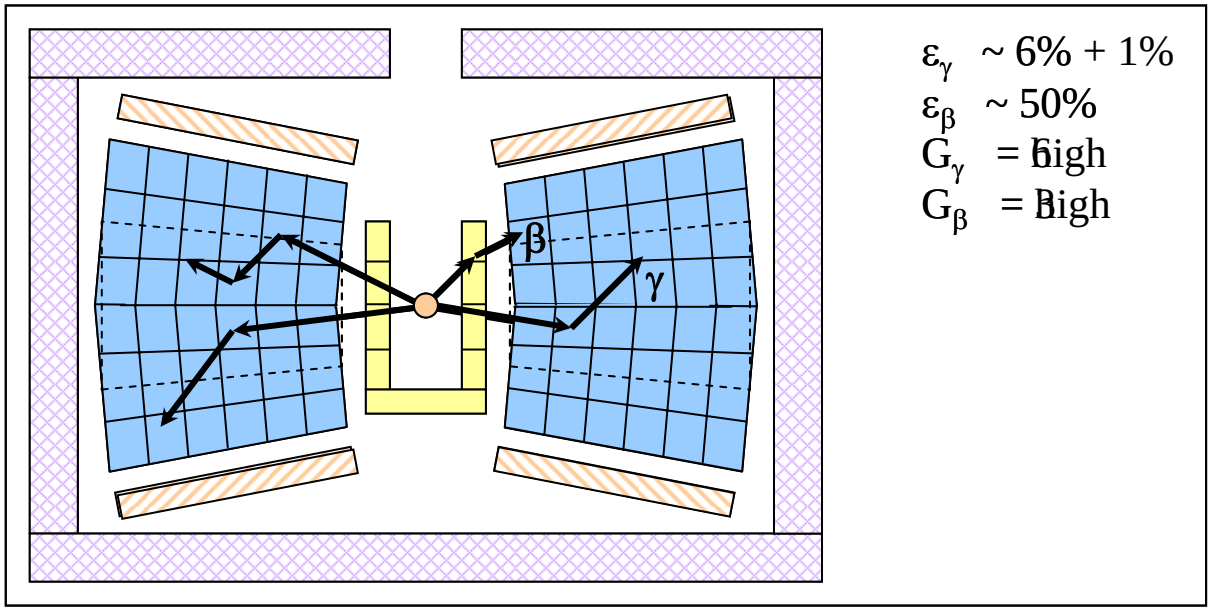

ε_γ ~ 6% + 1%
ε_β ~ 50%
G_γ = High
G_β = High

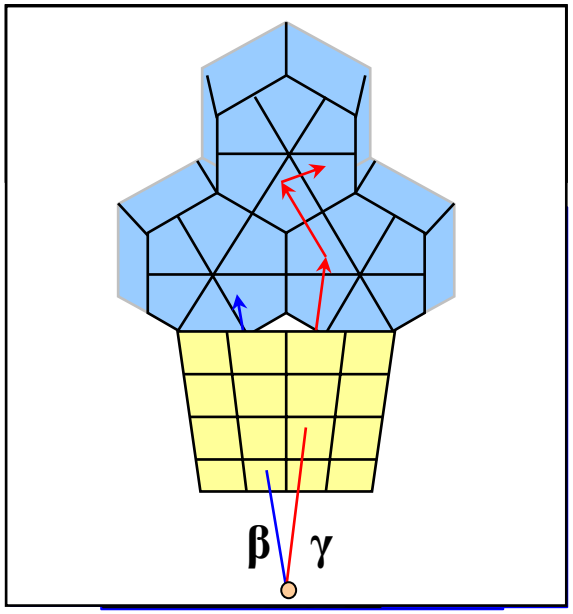

New β–γ-detection set-up at LISOL

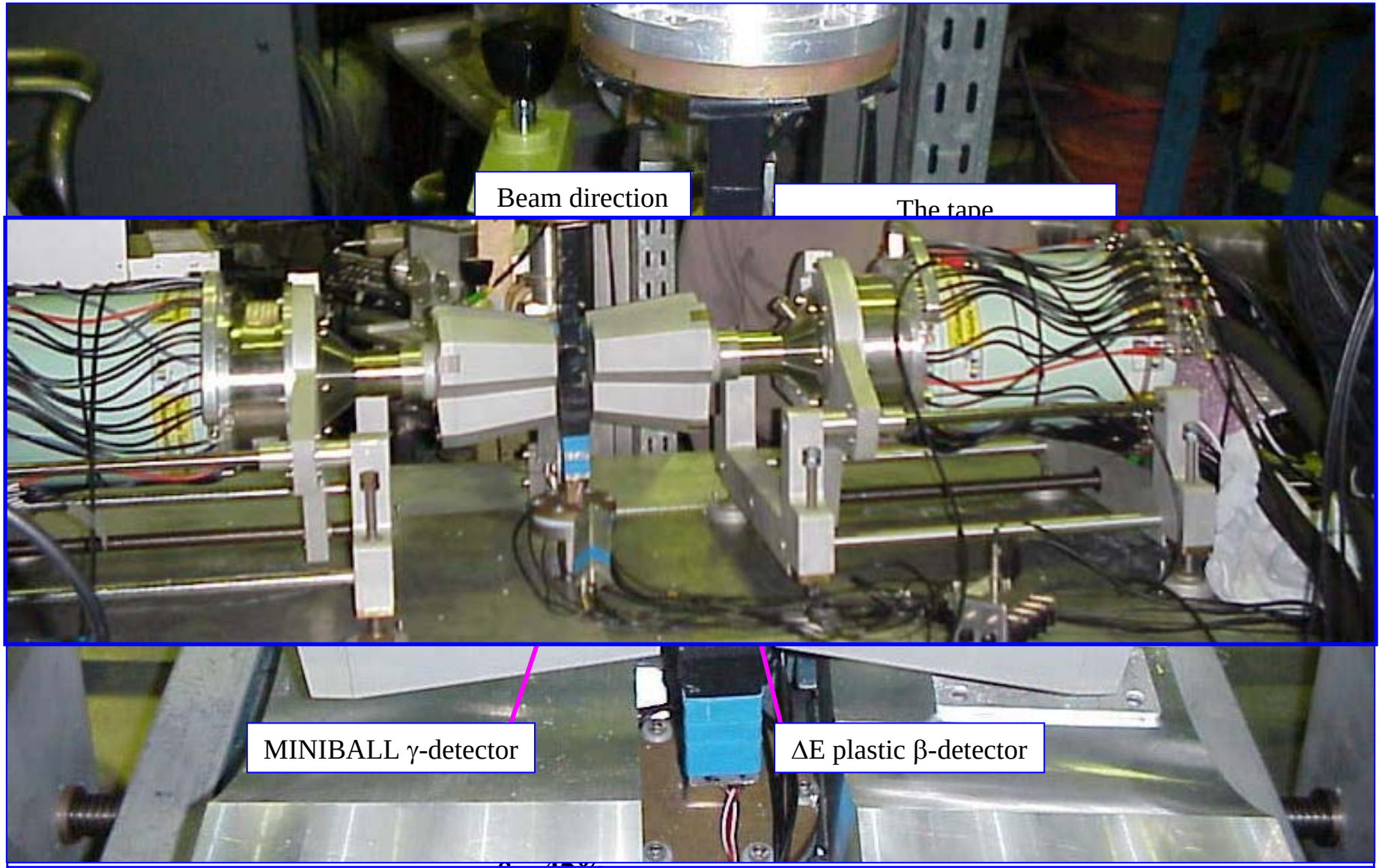

During experiments the detection set-up is shielded with *copper*, *lead,* and *borax*

Highly-segmented Hyper-pure Ge MINIBALL γ-detectors

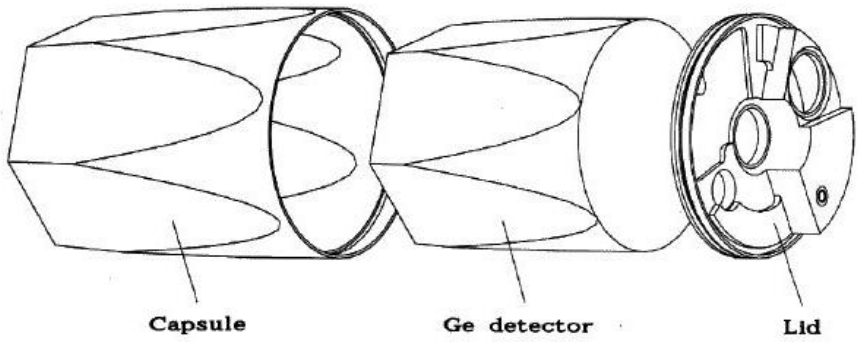

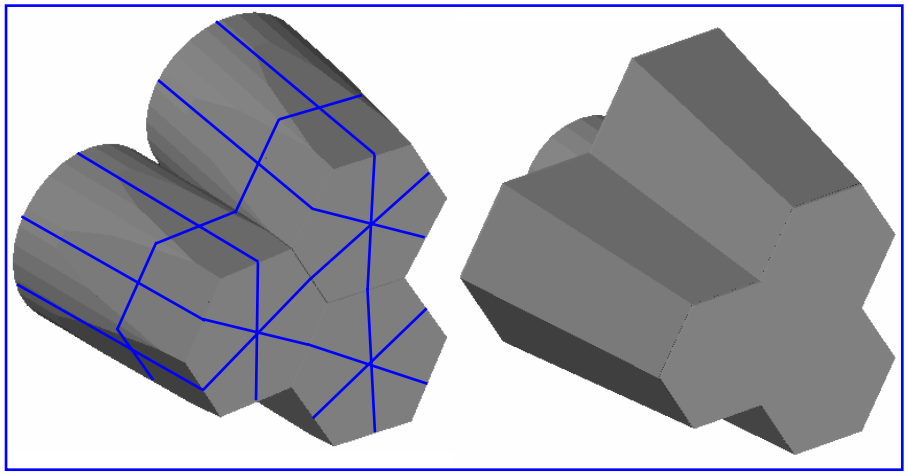

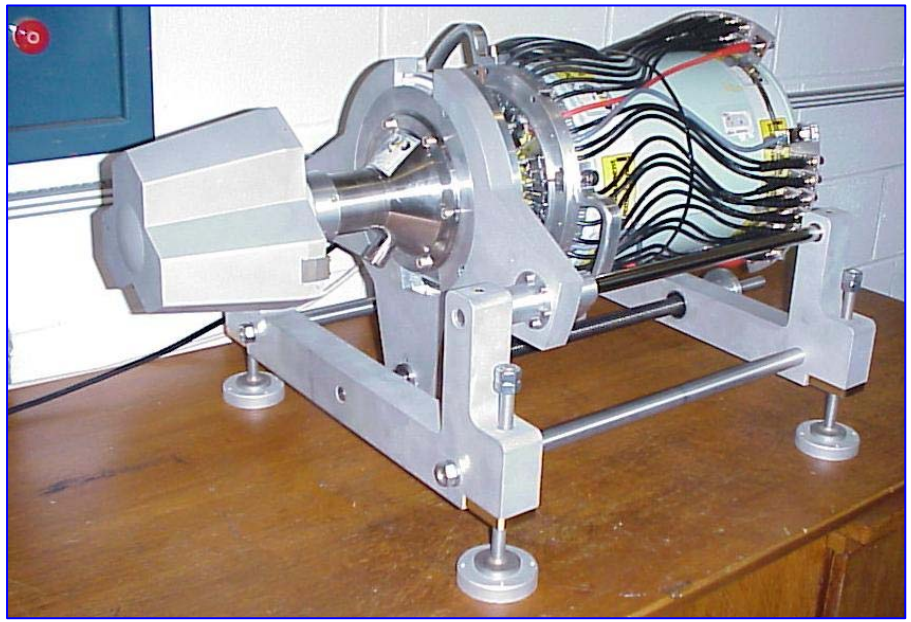

New 12-fold segmented MINIBALL triple-cluster detector

MINIBALL detector electronics

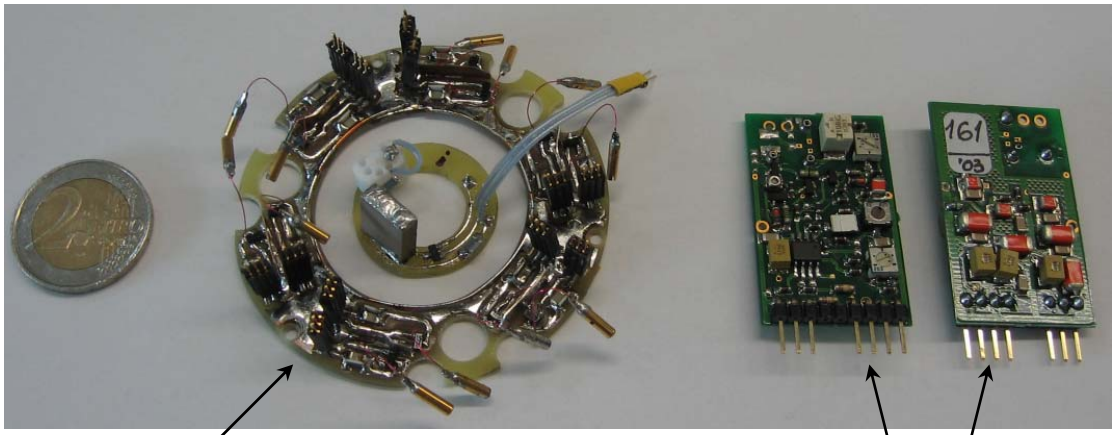

12-fold segmented cold preamplifier

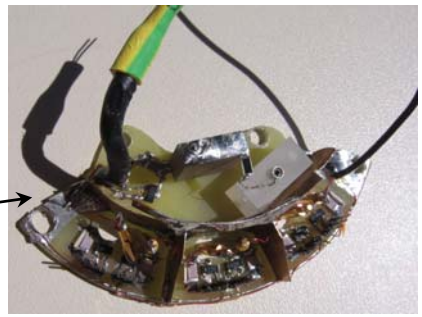

6-fold segmented cold preamplifier

Warm preamplifier

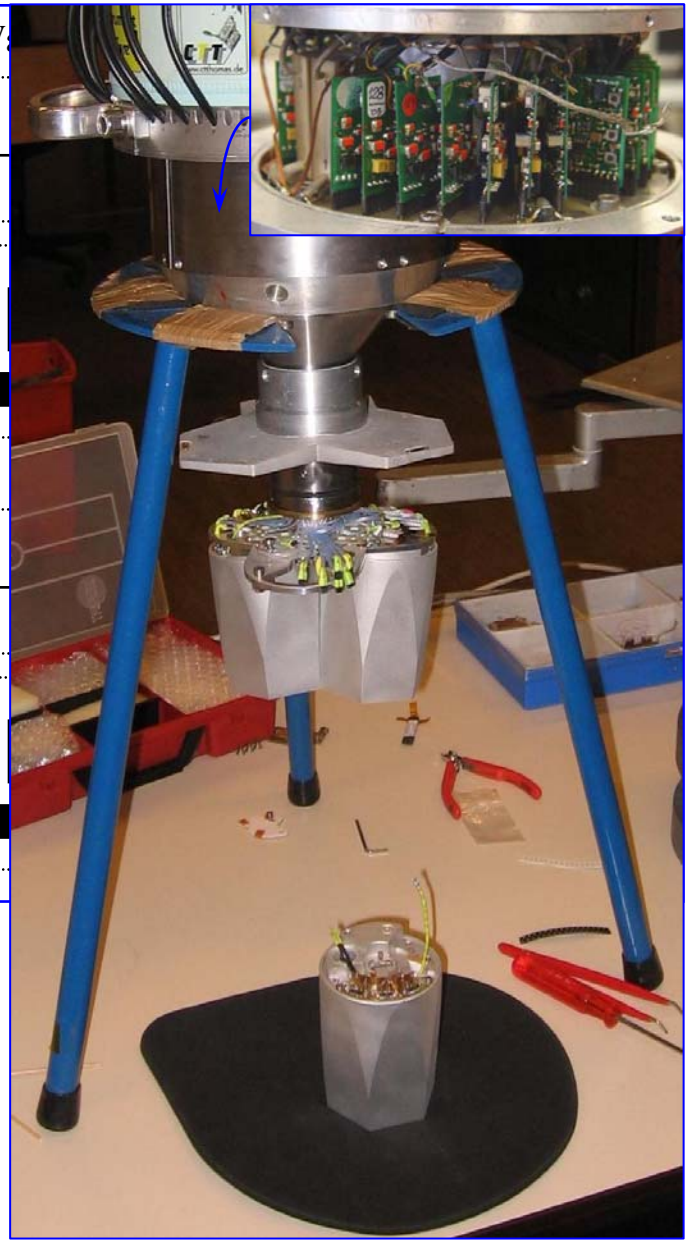

Developed by G. Pascovici, University of Cologne

(6+1) x 3 = 21 channels from 6-fold triple cluster
(12+1) x 3 = 39 channels from 12-fold triple cluster

Data-acquisition System

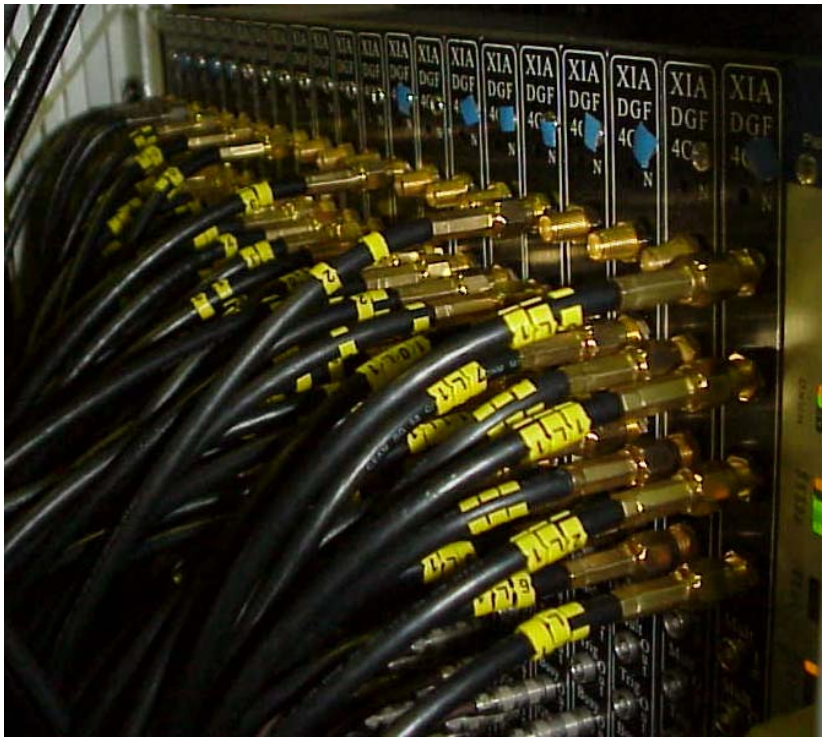

4 analogue signal inputs

Multiplicity In & Out

Trigger & Busy outputs

1-st & 2-nd level triggers

Clock synchronization

Main characteristics:

- ✓ 40 MHz sampling rate
- ✓ 16-bit ADC (65536 ch.)
- ✓ CAMAC interface
- ✓ Independent channels
- ✓ Implemented logics
- ✓ Clock synchronization
- ✓ On-board analysis
- ✓ Acquisition of all events
- ✓ Reduced dead time

Only recently the constant-fraction algorithm has been implemented
Pulse-shape analysis (on-line) or reconstruction algorithm (off-line) still to be done
$\Rightarrow$ The segment information has not been fully used yet

New data-analysis code, based on C++ and CERN Root package,
had to be written in order to analyze the acquired data

Pulse-shape Analysis

Same pulse height
⇒ all energy in 4

+ mirror charge
⇒ in 4, close to core

Pulse height of 3 > 5
⇒ in 4, close to 3

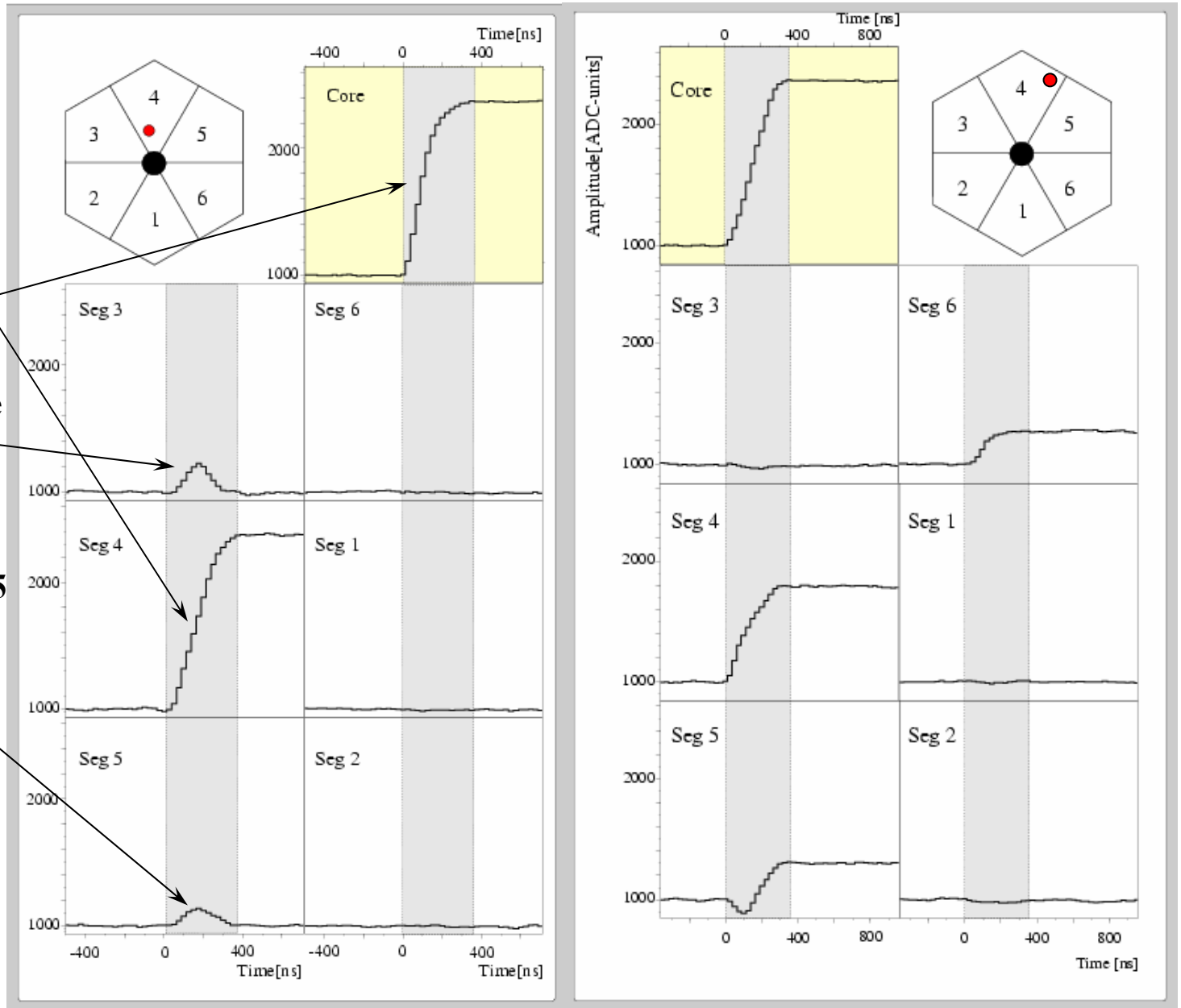

Event reconstruction

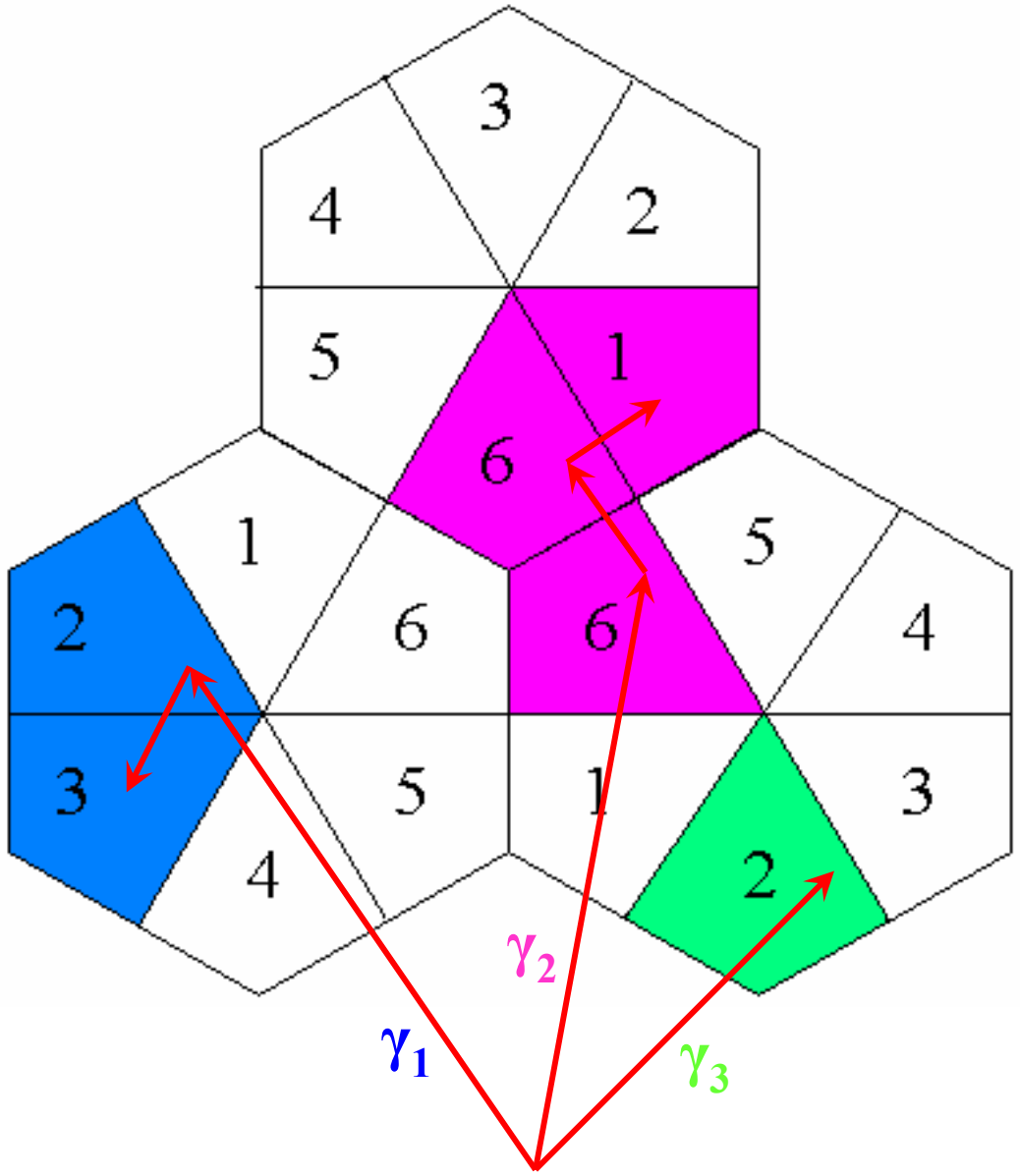

1. γ's scattered between crystals
2. γ's hitting the same crystal

3. Vetoing of incoming β's

4. Compton event shielding

5. Active background shielding

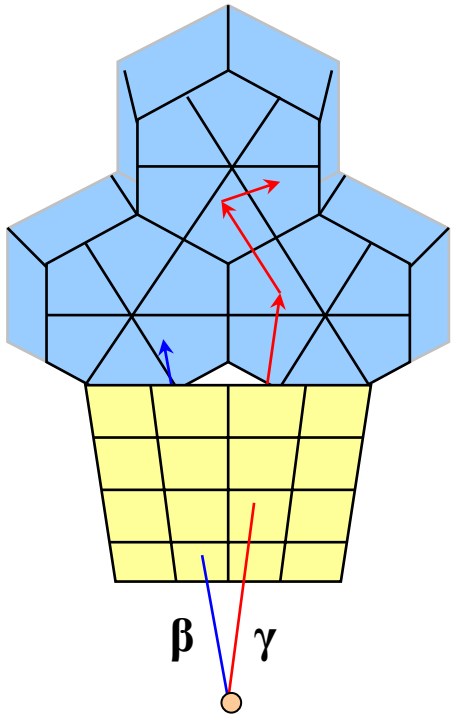

Results – β-decay of ^{65}Fe: βγ-coincidences

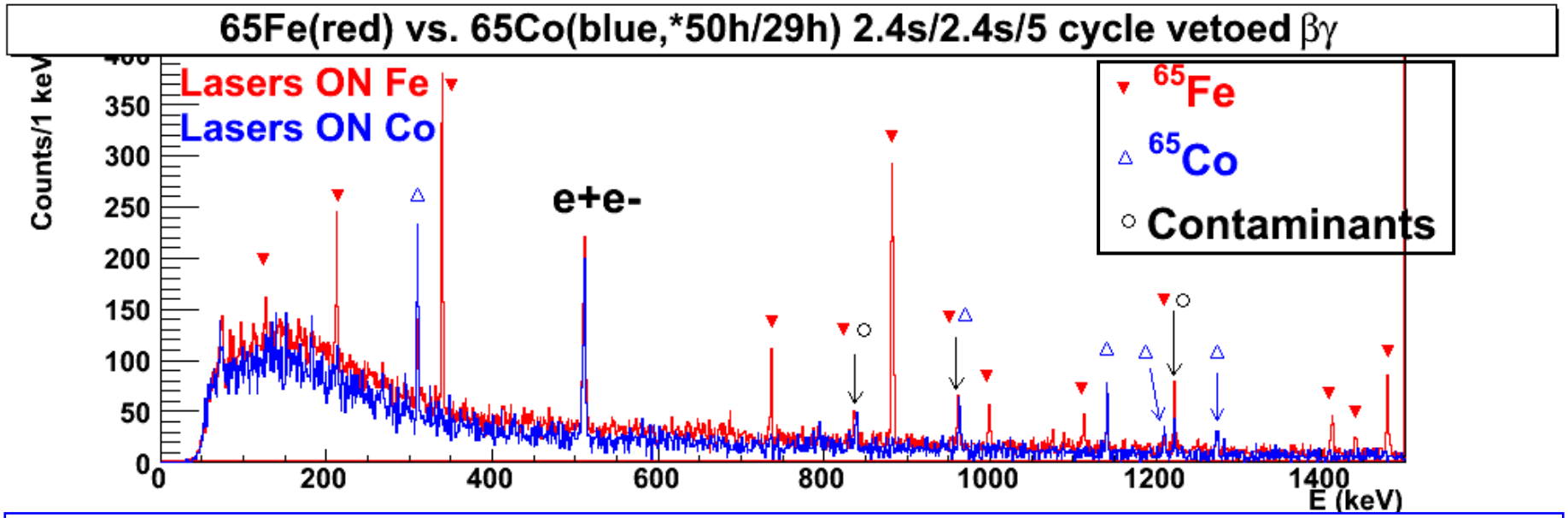

High production selectivity, low beam contamination, good detection selectivity

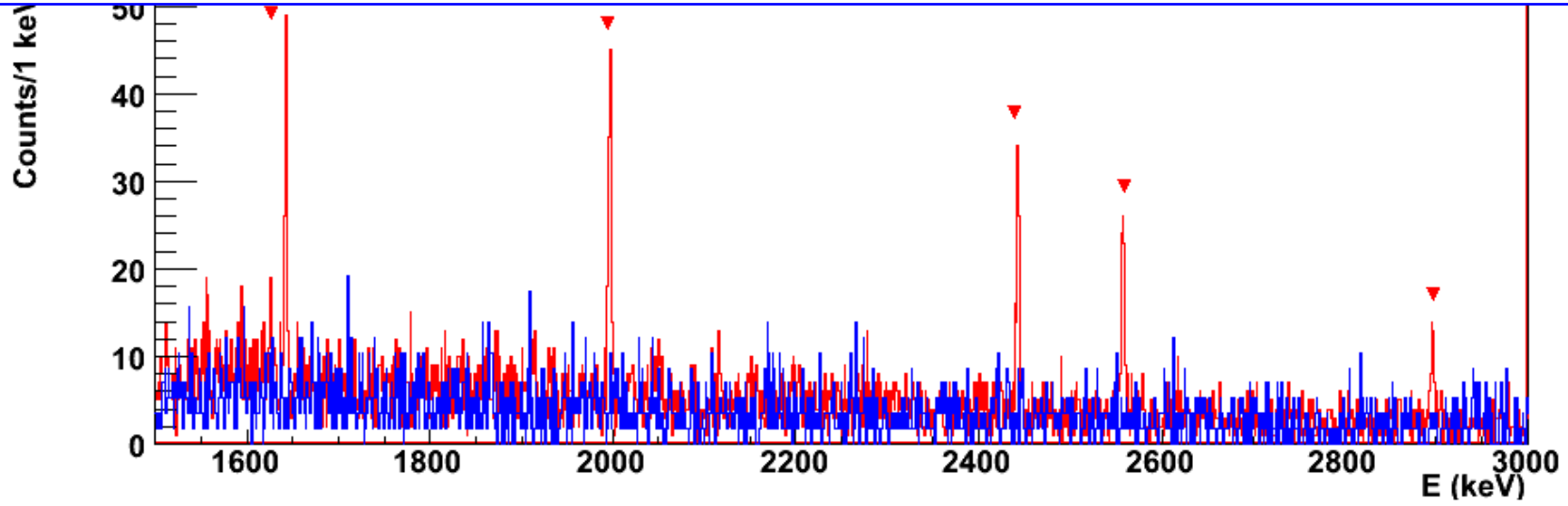

Results – β-decay of ^{66}Fe: βγγ-coincidences

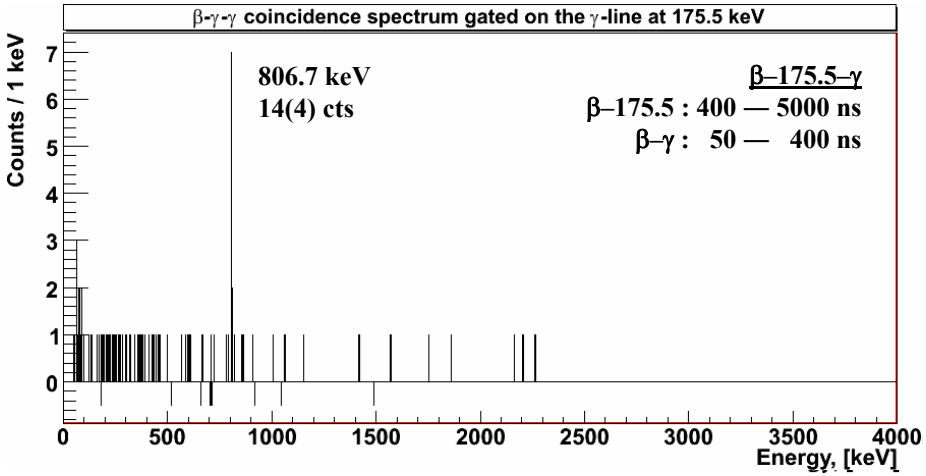

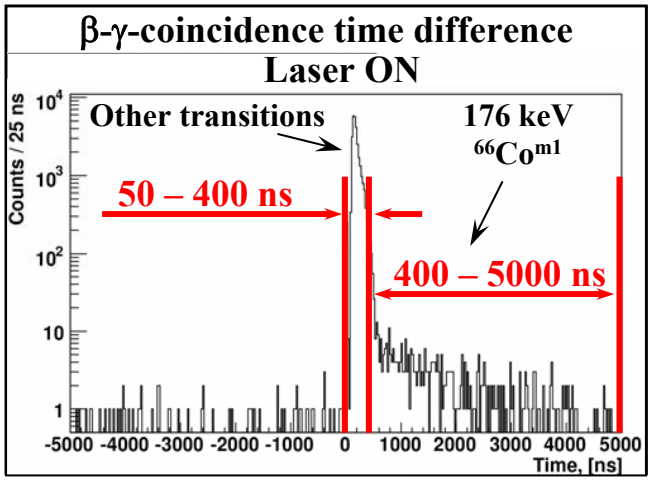

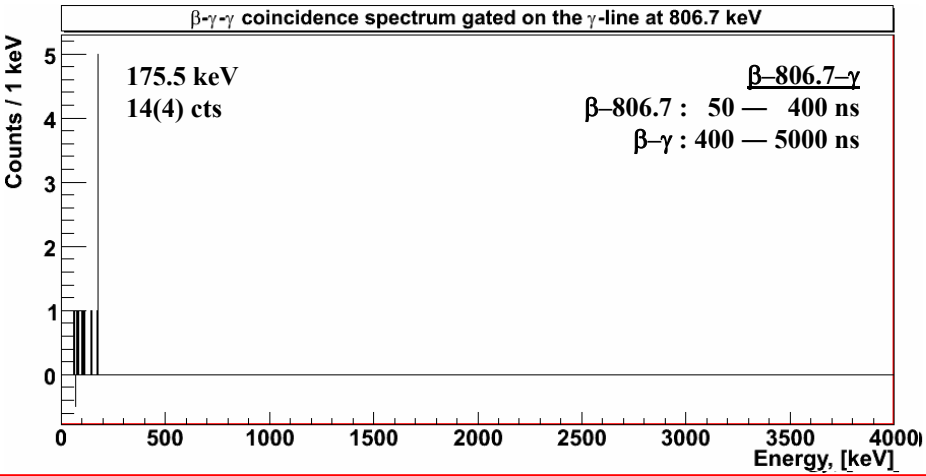

175.5 & 806.7 keV transitions are in cascade

175.5 & 806.7 keV transitions are in cascade, 806.7 keV is on top of 175.5 keV

Good detection selectivity ⇒ Low count-rate system

Results – β-decay of ^{66}Fe: half-life values

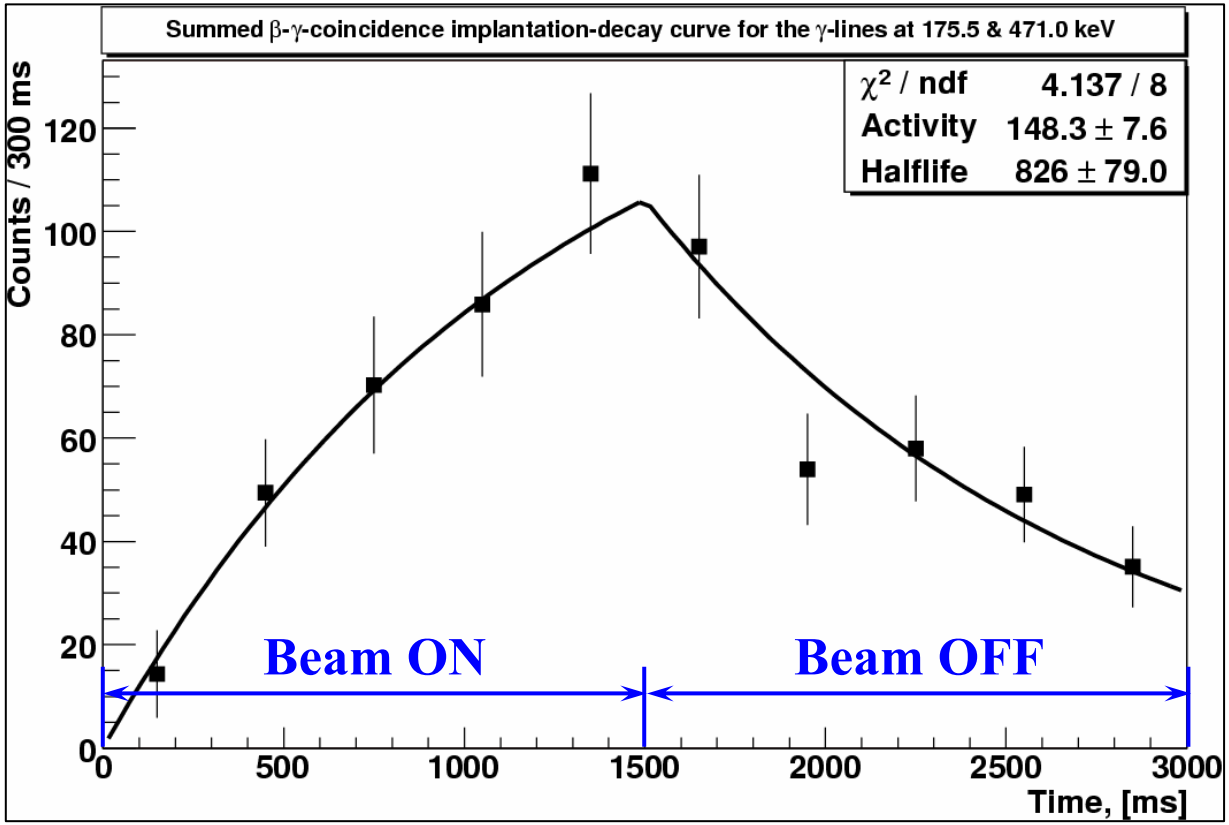

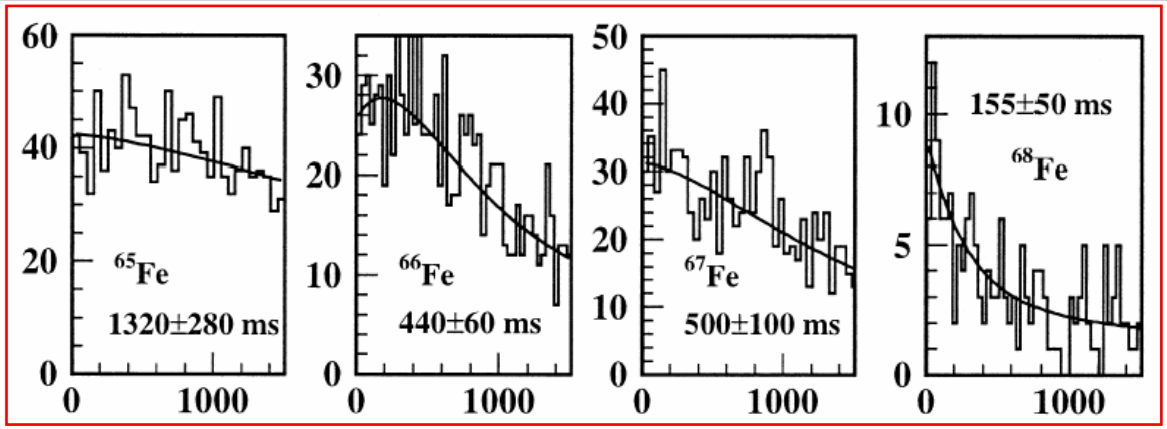

▪ ^{66}Fe

Leuven: 830 (80) ms

literature: 440 (60) ms

Sorlin *et al*, NPA 669 (2000)

Ameil *et al*, EPJ A 1 (1998)

Our method provides more reliable half-life values

Extracted from time behavior of single β-particles

Sorlin *et al*, NPA 669 (2000)

Results – β-decay of ^{67}Fe: event correlations

67Fe: 1.5 s / 1.5 s / 3 c, RED – lasers ON, BLUE – lasers OFF

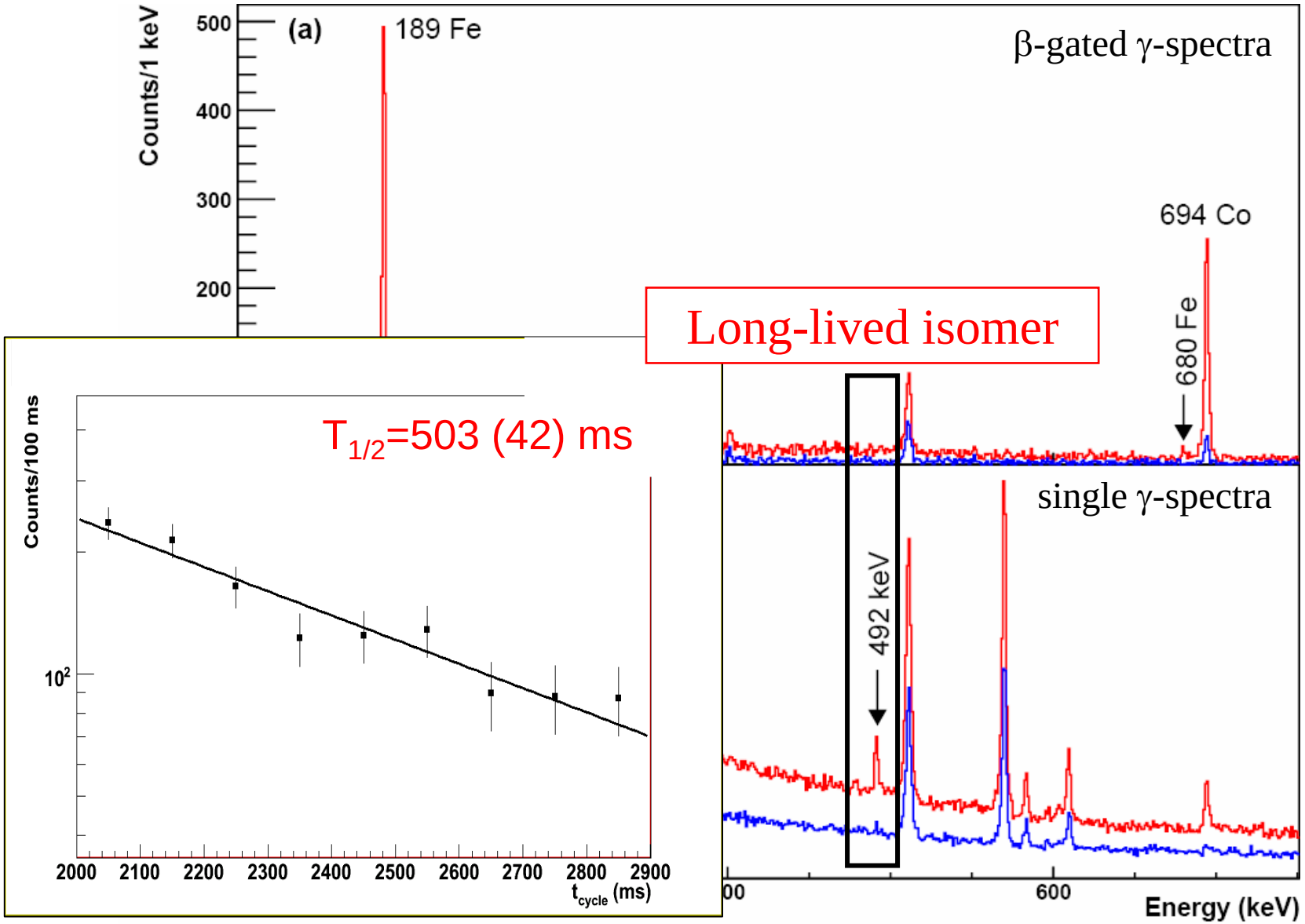

Results – β-decay of ^{67}Fe: event correlations

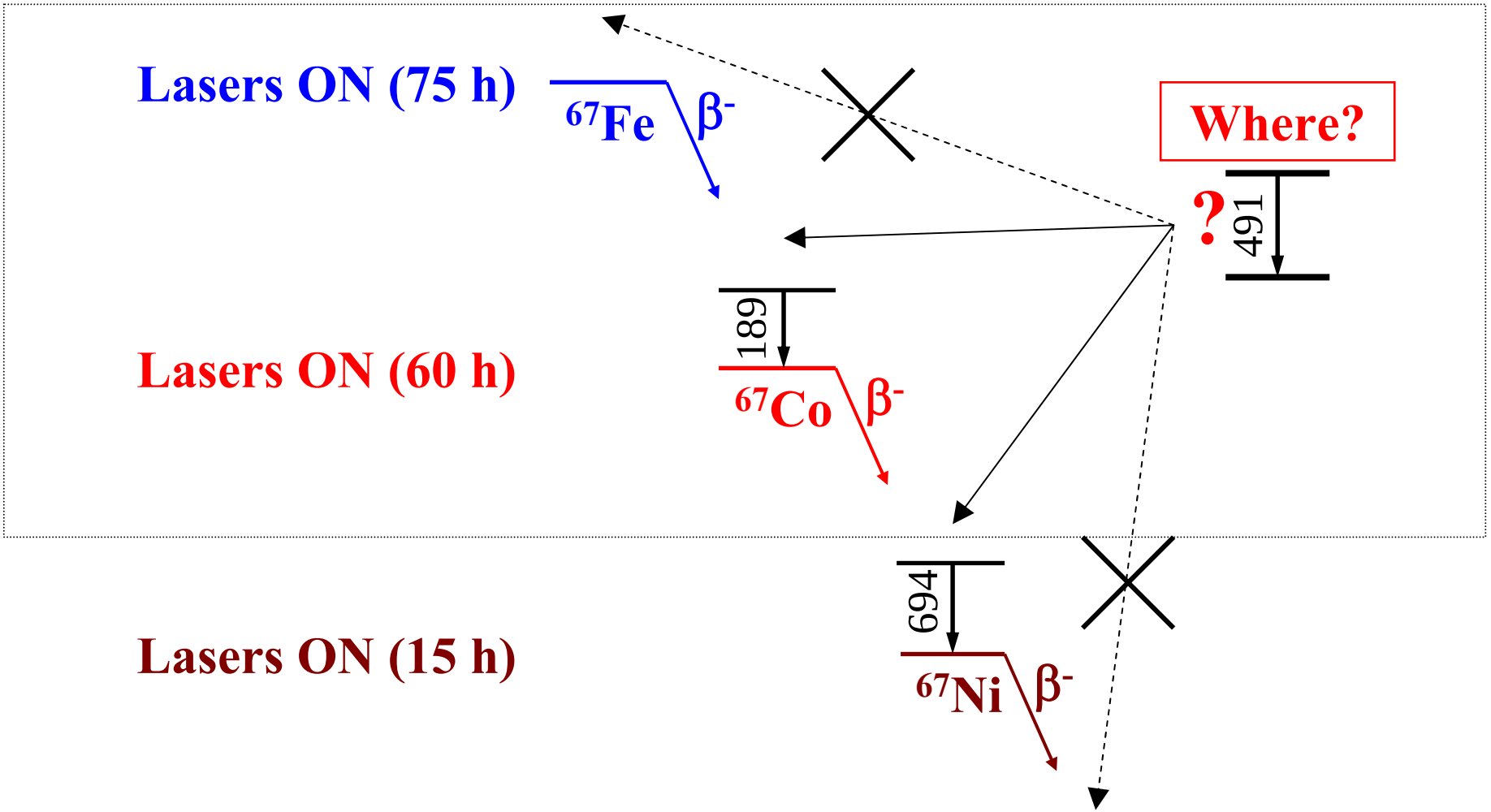

Digital electronics ⇒ Event-by-event data with time stamp ⇒ Event correlations!

Results – β-decay of ^{67}Fe: event correlations

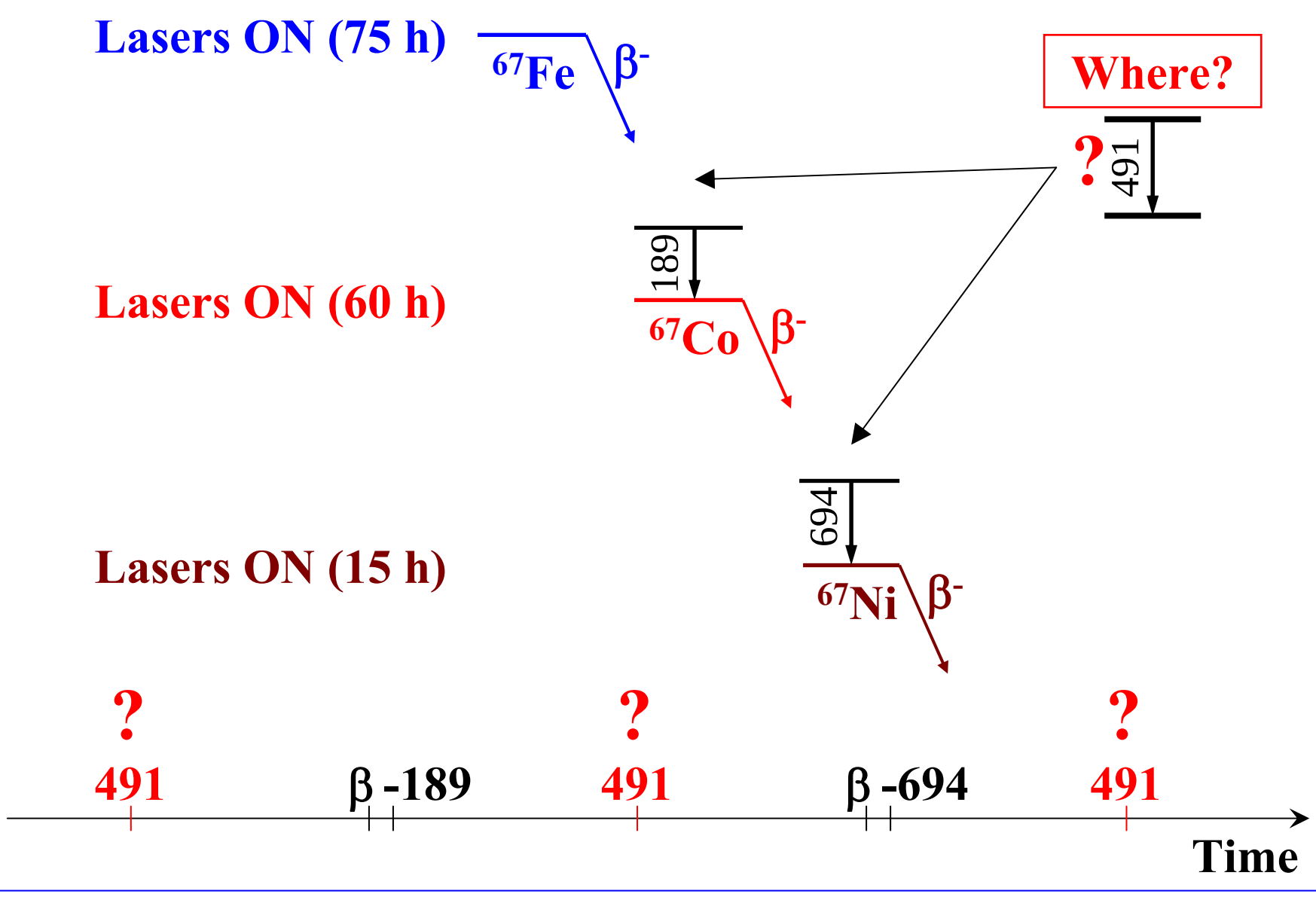

Results – β-decay of ^{67}Fe: event correlations

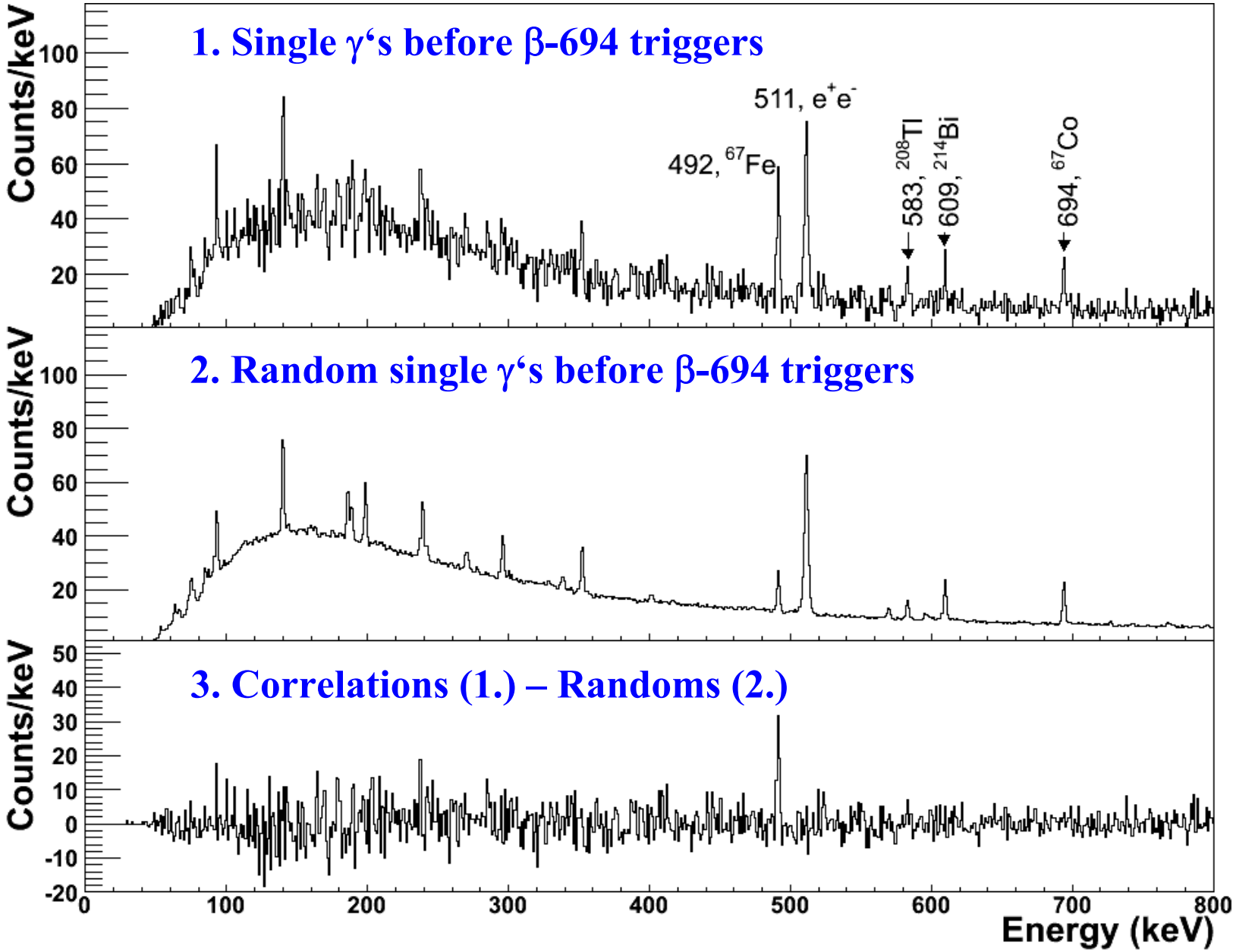

Results – β-decay of ^{67}Fe: event correlations

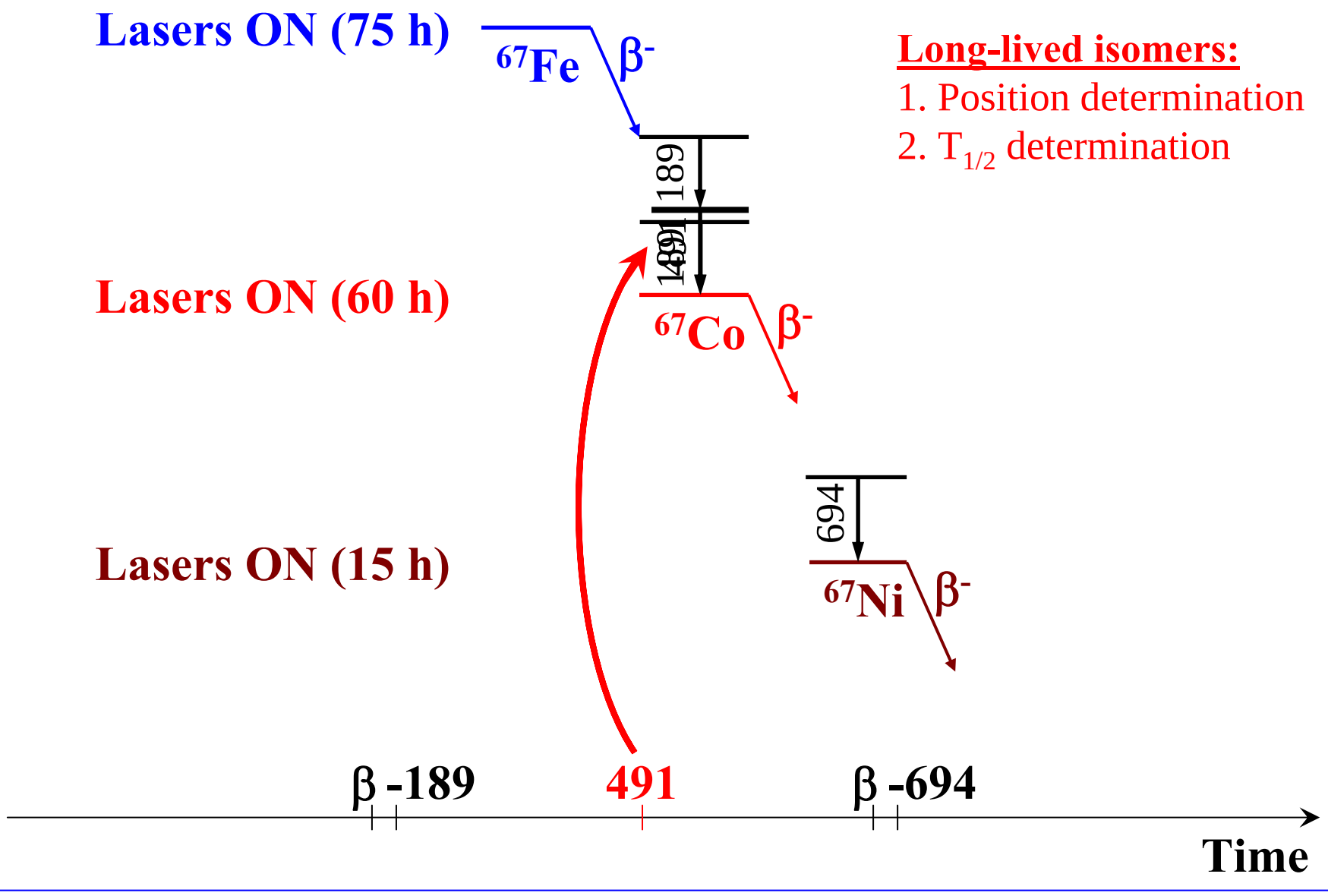

Long-lived isomers:

1. Position determination
2. $T_{1/2}$ determination

Conclusions

✓New β–γ-detection set-up has been constructed at LISOL:

- ➢ New 12-fold segmented MINIBALL triple cluster γ-detector assembled
- ➢ New data-acquisition system based on digital electronics introduced
- ➢ New data analysis approach

✓ β-decay studies of ^{65,66,67}Fe have been performed

Outlook

❖ Further work on the new β–γ-detection set-up:

- ➢ use of γ-segmentation: pulse-shape analysis and event reconstruction
- ➢ Introduction of segmented β-detectors
- ➢ Introduction of segmented active shielding

❖ Adapting to other facilities?

- ➢ β-decay studies at ILL? (at least logistics)
- ➢ β-decay studies at ISOLDE, CERN (24 shifts for $^{61\text{-}70}$Mn isotopes, Pb region)

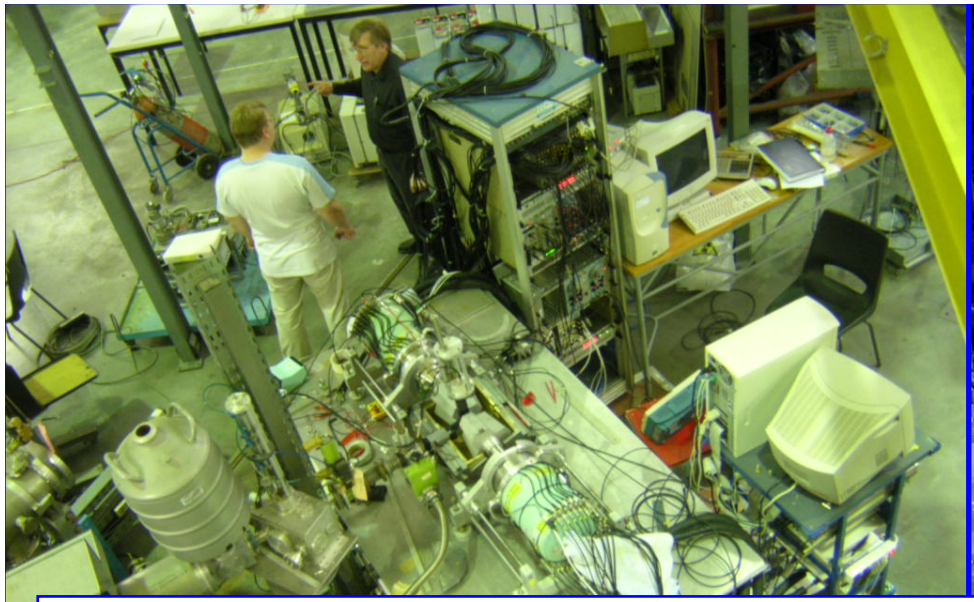

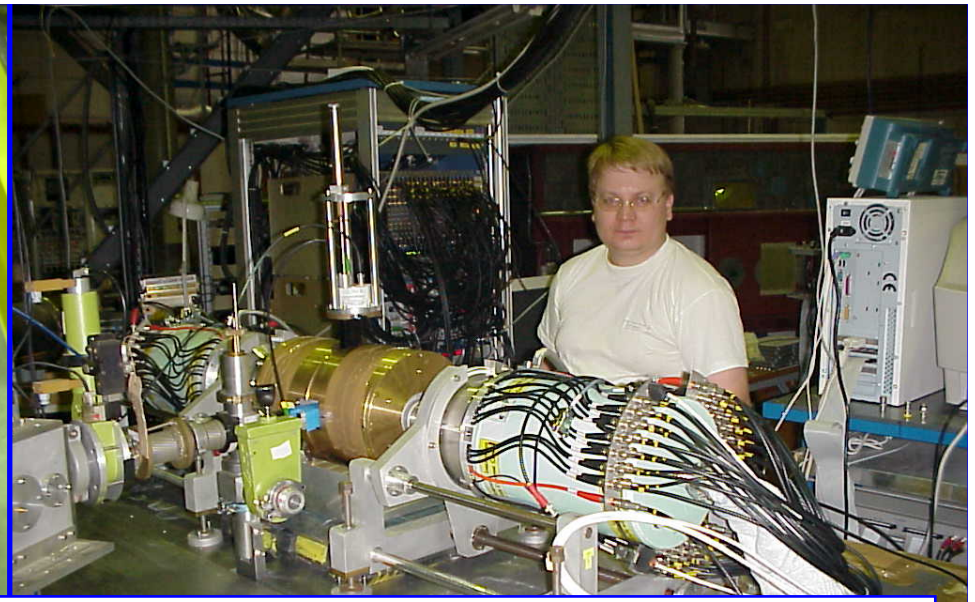

My *Sincere Gratitude* to the LISOL team
for productive COOPERATION & interesting WORK together!

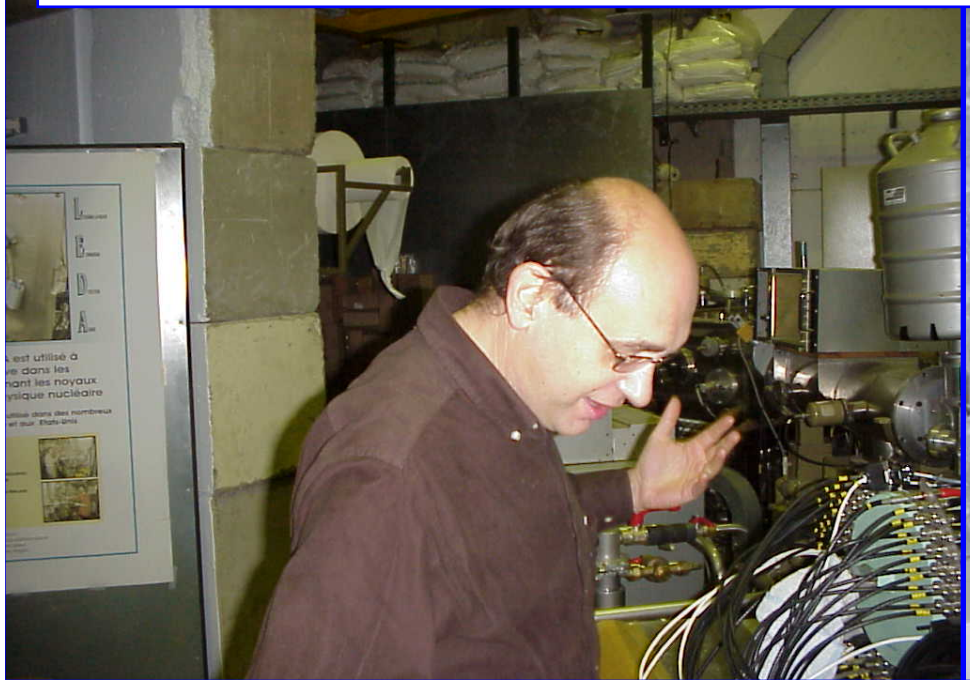

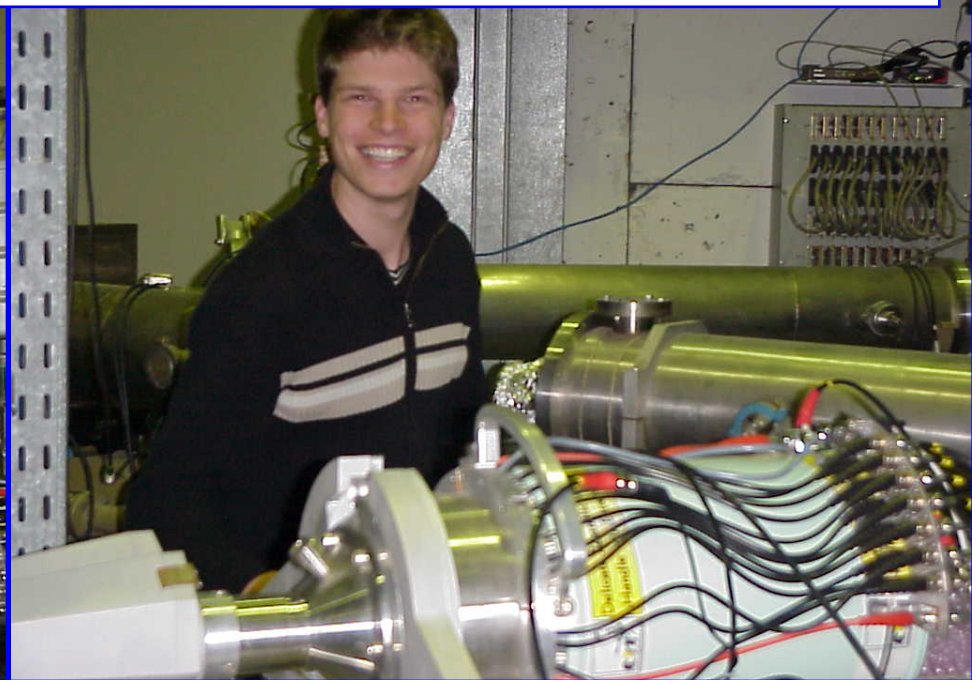

Results – ^{65}Fe: level scheme

From Penning trap mass measurements @ MSU (M. Block et al., submitted for PRL)

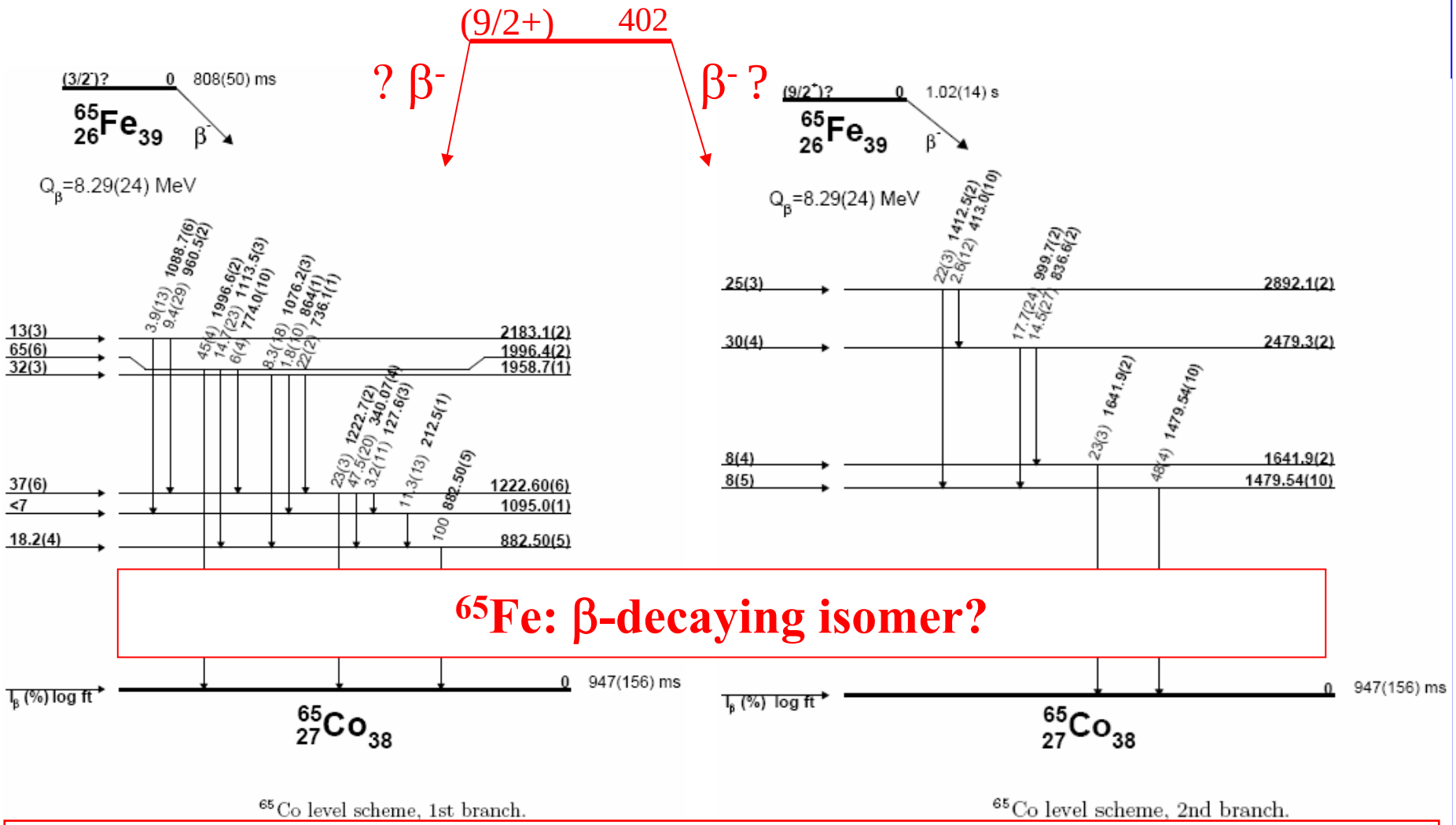

^{65}Co level scheme, 1st branch.

^{65}Co level scheme, 2nd branch.

^{65}Fe: β-decaying isomer?

Two independent branches: cannot be resolved on the half-life basis

Results – ^{66}Fe: level scheme

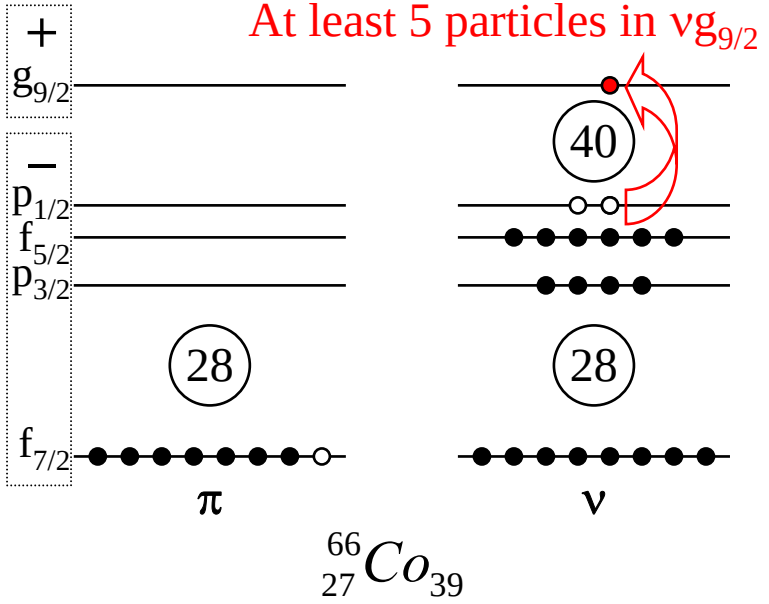

Paar's rule: Paar, NPA 331 (1979)

π–ν residual interaction ⇒ spin multiplet

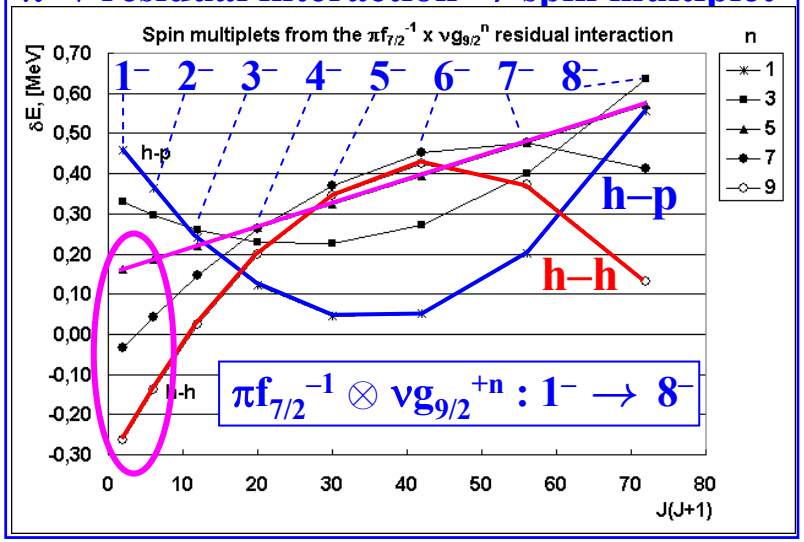

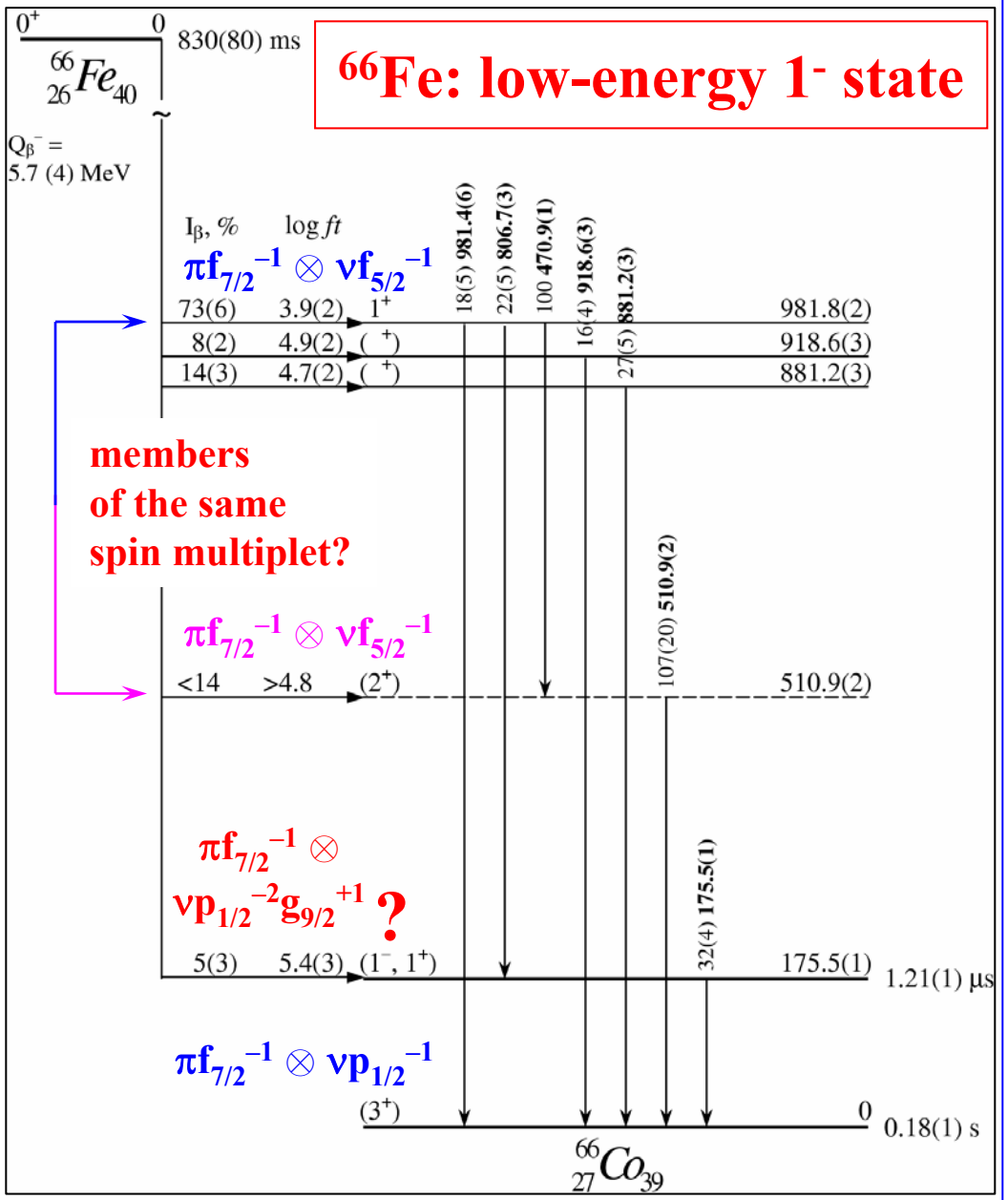

Results – ^{67}Fe: level scheme

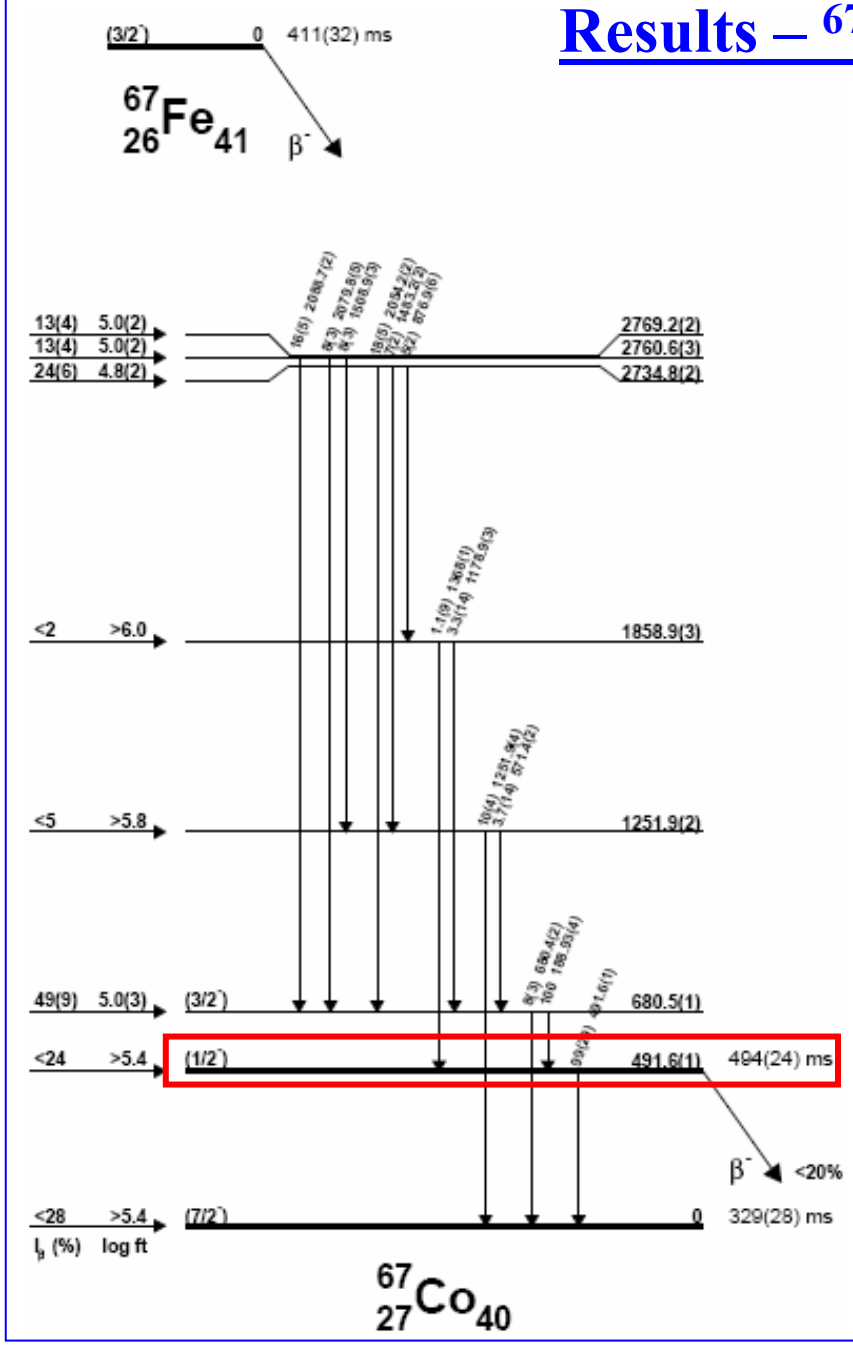

^{67}Fe: long-lived β-decaying isomer

Discussion – Nuclear structure of ^{66}Co: shape coexistence?

The presence of negative-parity states ⇒ occupation of the $\nu g_{9/2}$ orbital ⇒ deformation?

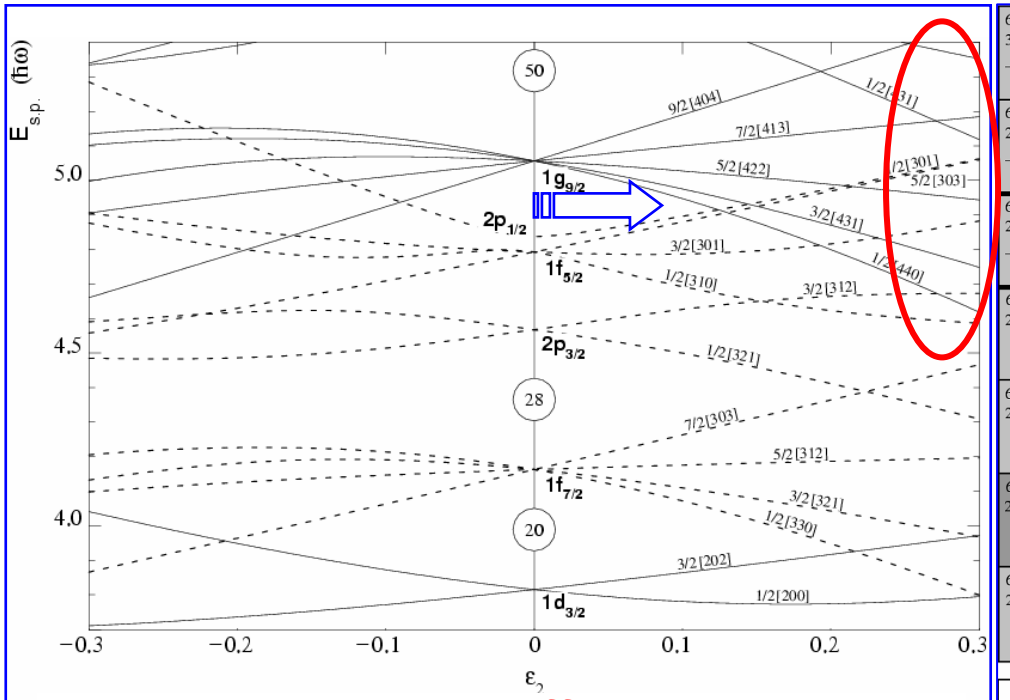

Possible scenario for ^{66}Co at $\beta \approx 0.30$:
occupation of the $\nu g_{9/2}$ orbital
Obliteration of N=40, Excitations across Z=28?

$^{66}_{30}$Zn$_{36}$ −0.20 0.22	$^{67}_{30}$Zn$_{37}$ −0.16	$^{68}_{30}$Zn$_{38}$ −0.17 0.21	$^{69}_{30}$Zn$_{39}$ −0.17	$^{70}_{30}$Zn$_{40}$ 0.24 0.23	$^{71}_{30}$Zn$_{41}$ 0.26	$^{72}_{30}$Zn$_{42}$ 0.23 0.23	$^{73}_{30}$Zn$_{43}$ 0.23	$^{74}_{30}$Zn$_{44}$ 0.20 0.25
$^{65}_{29}$Cu$_{36}$ −0.17	$^{66}_{29}$Cu$_{37}$ −0.16	$^{67}_{29}$Cu$_{38}$ −0.16	$^{68}_{29}$Cu$_{39}$ −0.16	$^{69}_{29}$Cu$_{40}$ 0.08	$^{70}_{29}$Cu$_{41}$ 0.11	$^{71}_{29}$Cu$_{42}$ 0.12	$^{72}_{29}$Cu$_{43}$ 0.12	$^{73}_{29}$Cu$_{44}$ 0.14
$^{64}_{28}$Ni$_{36}$ −0.17 0.18	$^{65}_{28}$Ni$_{37}$ −0.12	$^{66}_{28}$Ni$_{38}$ −0.12 0.16	$^{67}_{28}$Ni$_{39}$ −0.08	$^{68}_{28}$Ni$_{40}$ 0.01 0.10	$^{69}_{28}$Ni$_{41}$ −0.05	$^{70}_{28}$Ni$_{42}$ 0.01 0.18	$^{71}_{28}$Ni$_{43}$ 0.05	$^{72}_{28}$Ni$_{44}$ 0.05
$^{63}_{27}$Co$_{36}$ 0.15	$^{64}_{27}$Co$_{37}$ 0.14	$^{65}_{27}$Co$_{38}$ 0.14	$^{66}_{27}$Co$_{39}$ 0.09 ?	$^{67}_{27}$Co$_{40}$ 0.14 ?	$^{68}_{27}$Co$_{41}$ 0.13 ?	$^{69}_{27}$Co$_{42}$ 0.16	$^{70}_{27}$Co$_{43}$ 0.17	$^{71}_{27}$Co$_{44}$ 0.16
$^{62}_{26}$Fe$_{36}$ 0.18	$^{63}_{26}$Fe$_{37}$ 0.15	$^{64}_{26}$Fe$_{38}$ 0.24	$^{65}_{26}$Fe$_{39}$ 0.30	$^{66}_{26}$Fe$_{40}$ 0.27	$^{67}_{26}$Fe$_{41}$ 0.30	$^{68}_{26}$Fe$_{42}$ 0.26	$^{69}_{26}$Fe$_{43}$ 0.27	$^{70}_{26}$Fe$_{44}$ 0.23
$^{61}_{25}$Mn$_{36}$ 0.23	$^{62}_{25}$Mn$_{37}$ 0.24	$^{63}_{25}$Mn$_{38}$ 0.26	$^{64}_{25}$Mn$_{39}$ 0.30	$^{65}_{25}$Mn$_{40}$ 0.28	$^{66}_{25}$Mn$_{41}$ 0.29	$^{67}_{25}$Mn$_{42}$ 0.28	$^{68}_{25}$Mn$_{43}$ 0.28	$^{69}_{25}$Mn$_{44}$ 0.24
$^{60}_{24}$Cr$_{36}$ 0.17	$^{61}_{24}$Cr$_{37}$ 0.14	$^{62}_{24}$Cr$_{38}$ 0.28	$^{63}_{24}$Cr$_{39}$ 0.31	$^{64}_{24}$Cr$_{40}$ 0.28	$^{65}_{24}$Cr$_{41}$ 0.30	$^{66}_{24}$Cr$_{42}$ 0.27	$^{67}_{24}$Cr$_{43}$ 0.29	$^{68}_{24}$Cr$_{44}$ 0.26

Absolute value of the quadrupole deformation parameter β_2
□ 0.00 – 0.10
□ 0.11 – 0.20
□ 0.21 – 0.30
□ 0.31 – 0.40
◥ stable

Aboussir et al, At.Data Tables 61, (1995)
Raman et al, At.Data Tables 78, (2001)

Ground state of ^{66}Fe is deformed: $\beta \approx 0.30$ (Hannawald et al, PRL 82 (1999) / experiment /)

Ground state of ^{66}Co is spherical: $\beta = 0.09$ (Aboussir et al, At. Data Tables 61 (1995) / theory /)

^{66}Co: 1^- deformed, 3^+ spherical — ***Shape coexistence in ^{66}Co?***

Nuclear structure of nuclei in the neutron-rich Ni region

Main Physics Goals

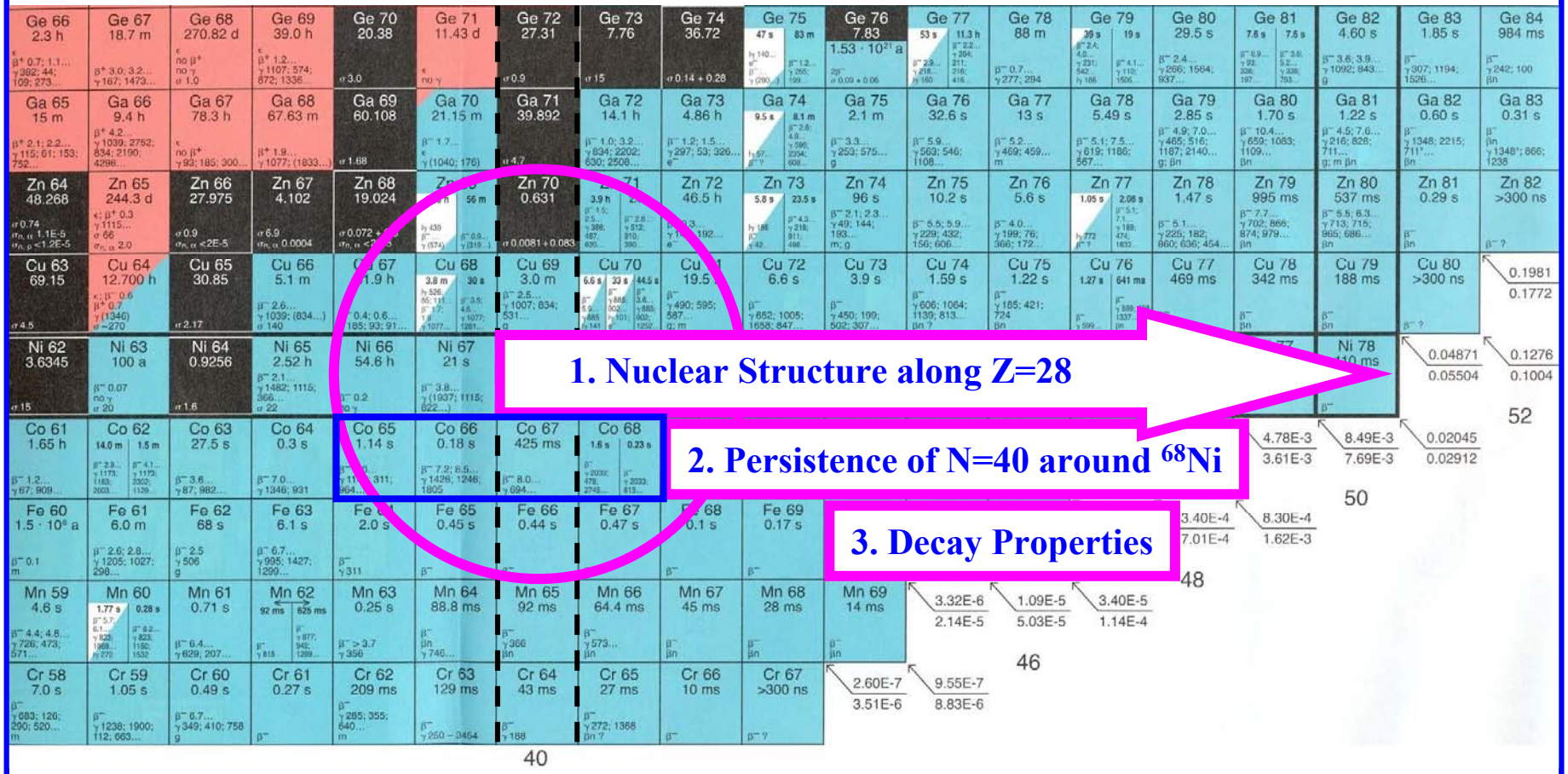

The specific physics goal of this project is
the nuclear structure of neutron-rich Co nuclides in the vicinity of ^{68}Ni

Nuclear Structure around semi-doubly magic ^{68}Ni

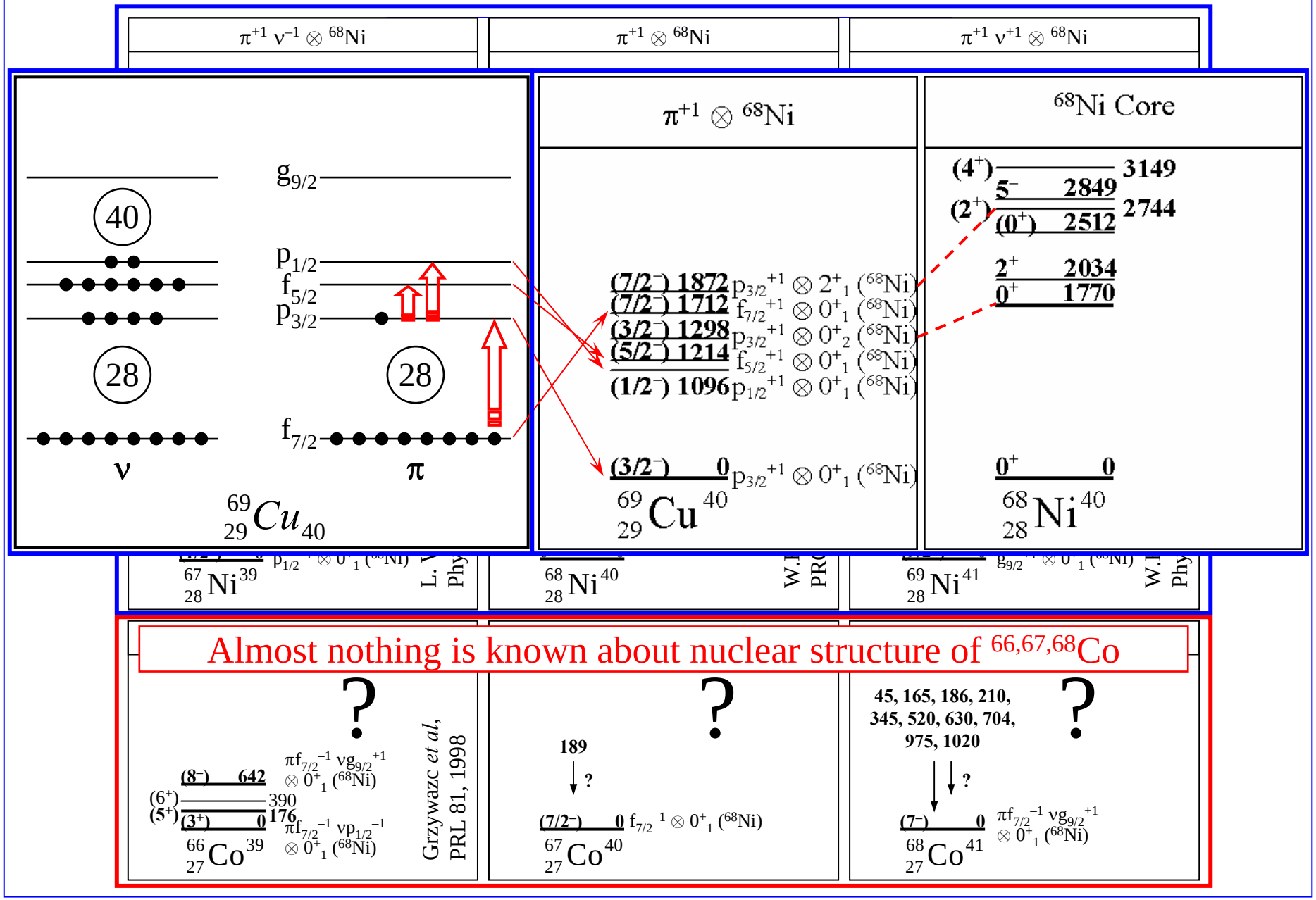

Nuclear Structure around semi-doubly magic ^{68}Ni

Fe, Co, Ni are refractory-type elements ⇒
Most studies were done using In-Flight separation method

No extensive β-decay studies were performed for Fe nuclei

Decay properties: Half-lives extracted from time behavior of single β-particles
Sorlin *et al*, NPA 669 (2000)

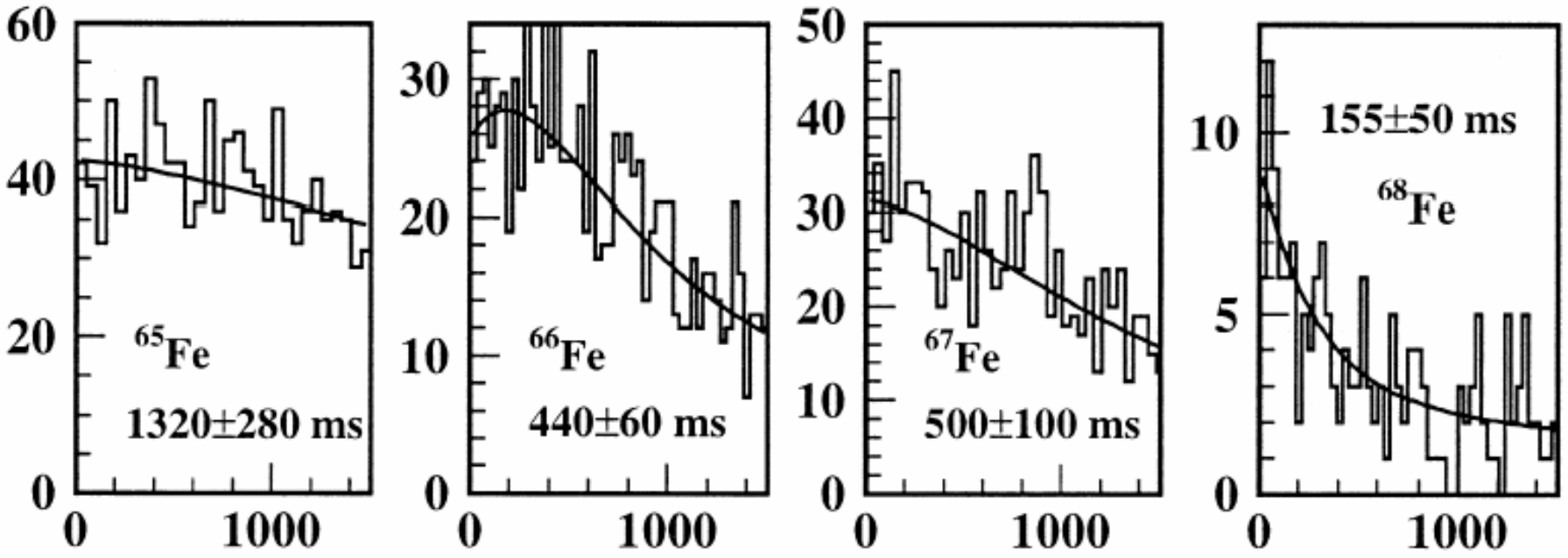

Nuclear structure of Co nuclei
can be successfully studied
in β⁻-decay of Fe isobars

stable

Tables 78, (2001)

Possible ground-state deformation

Experimental Setup: proton-induced fission of ^{238}U at LISOL

Leuven Isotope Separator-On-Line

- Element Separation
- Mass Separation (A/q)
- Relatively Fast

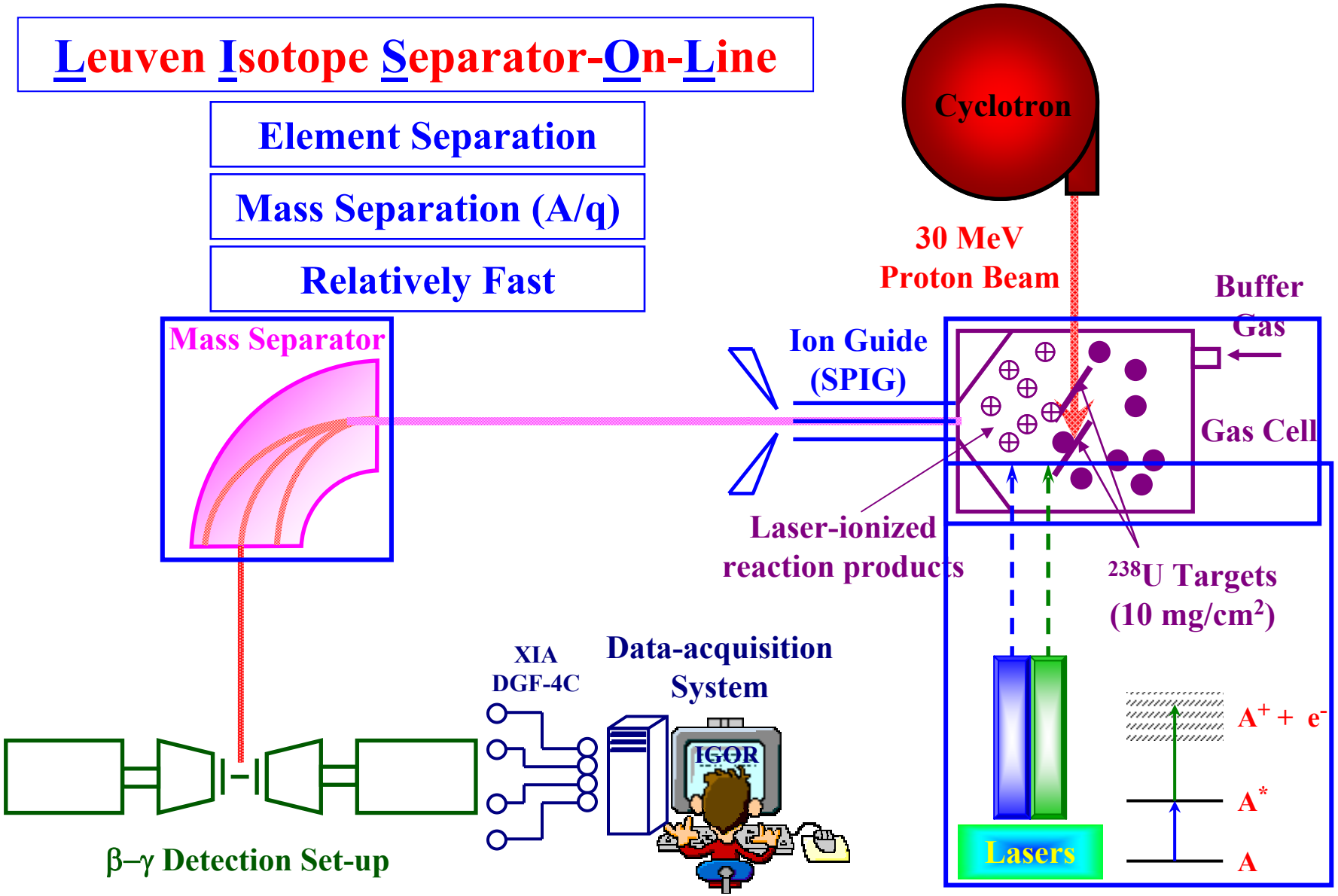

Experimental Setup: The LISOL Facility in Louvain-La-Neuve

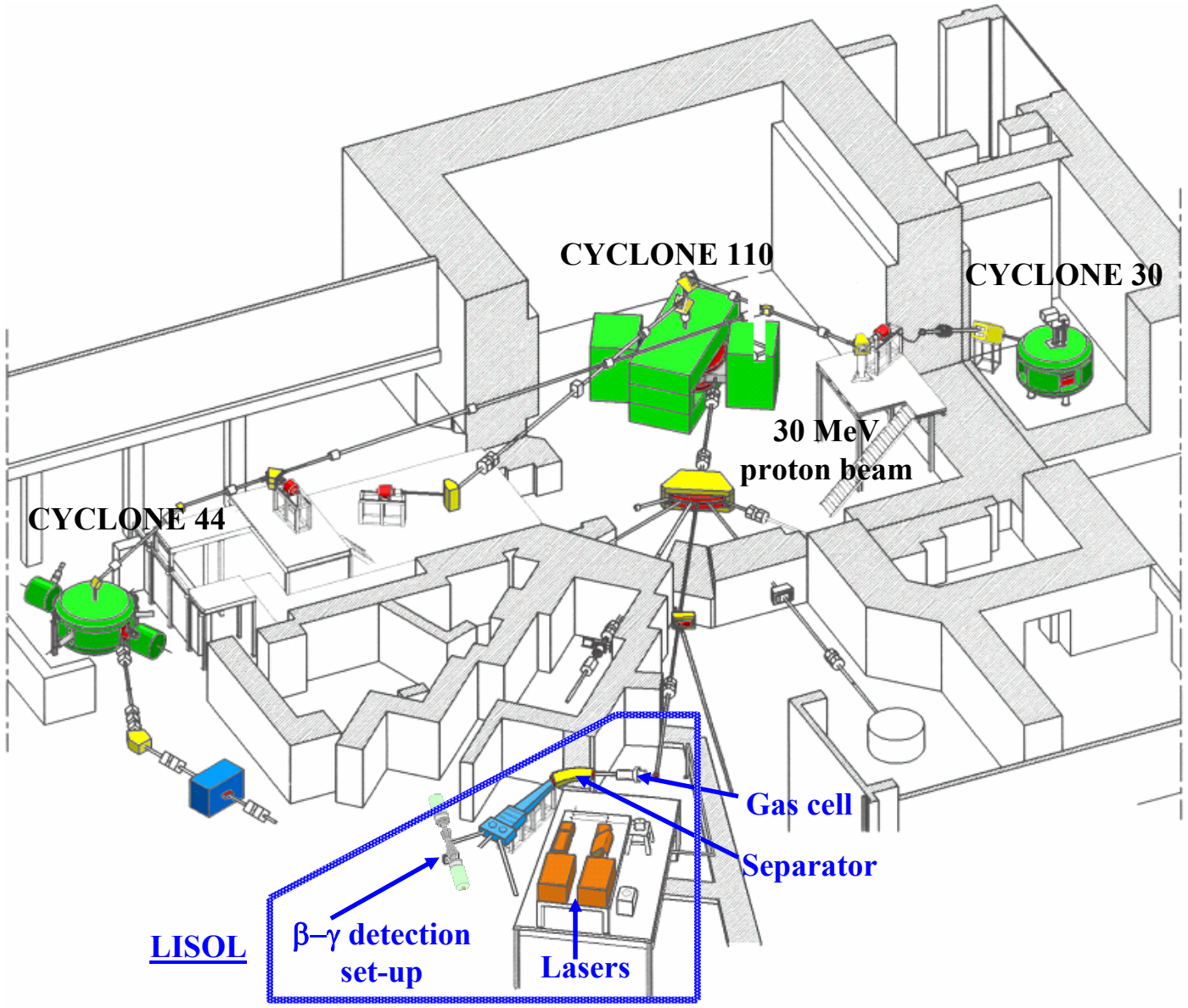

Results – β-decay of ^{66}Fe: β-gated γ-spectra

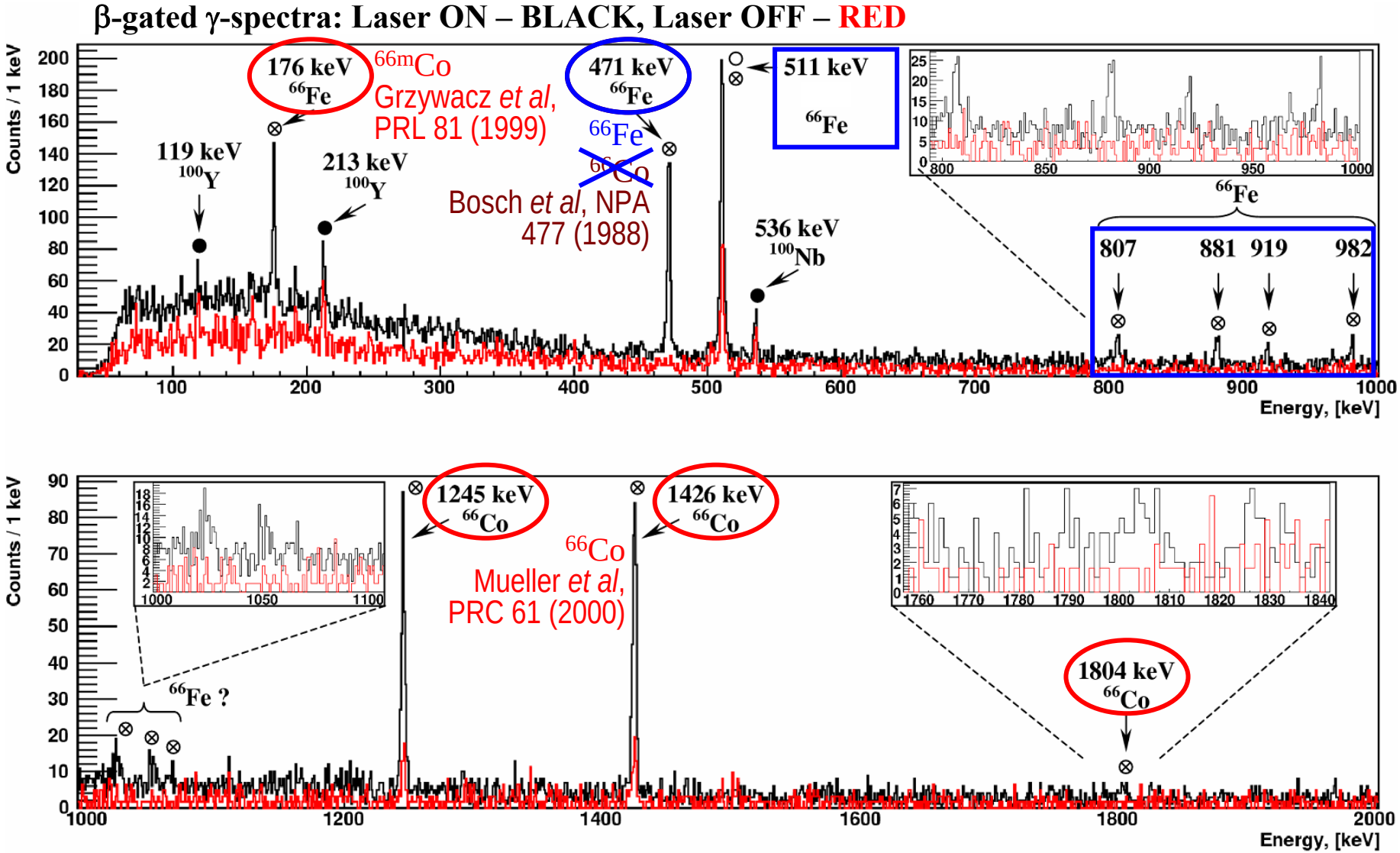

New γ-transitions from the decay of ^{66}Fe were identified

Results – β-decay of ^{66}Fe: βγγ-coincidences

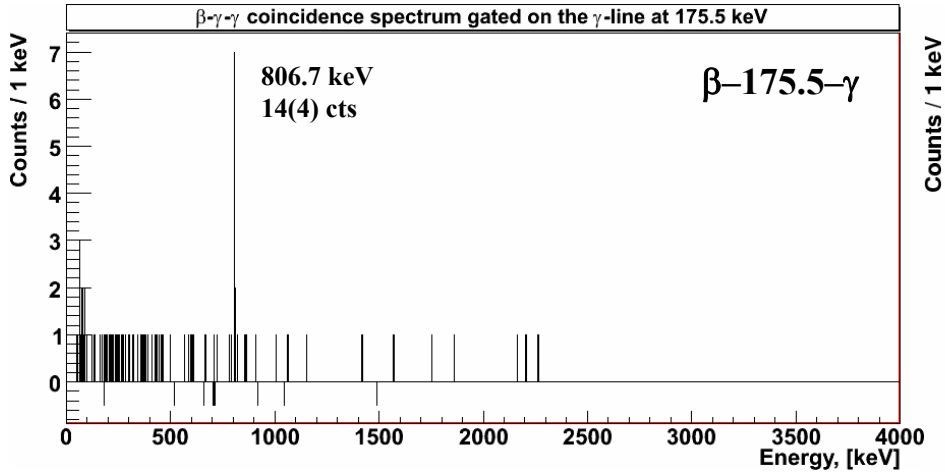

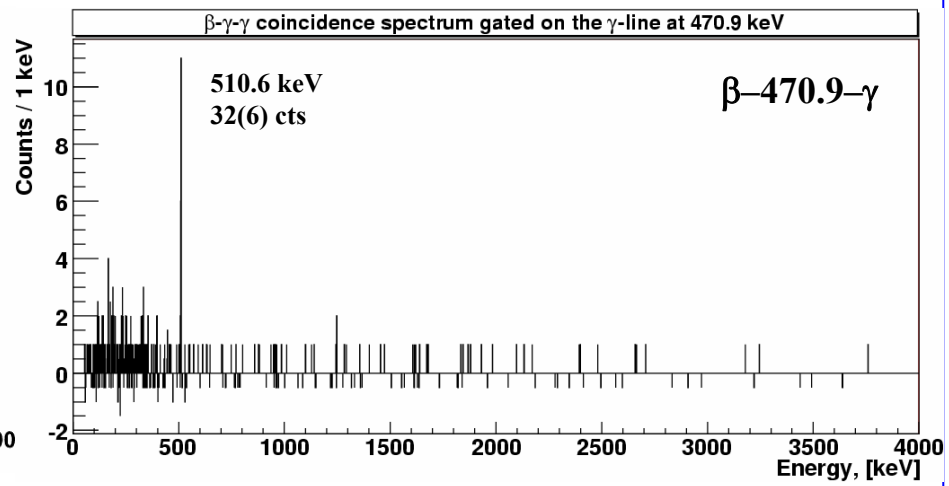

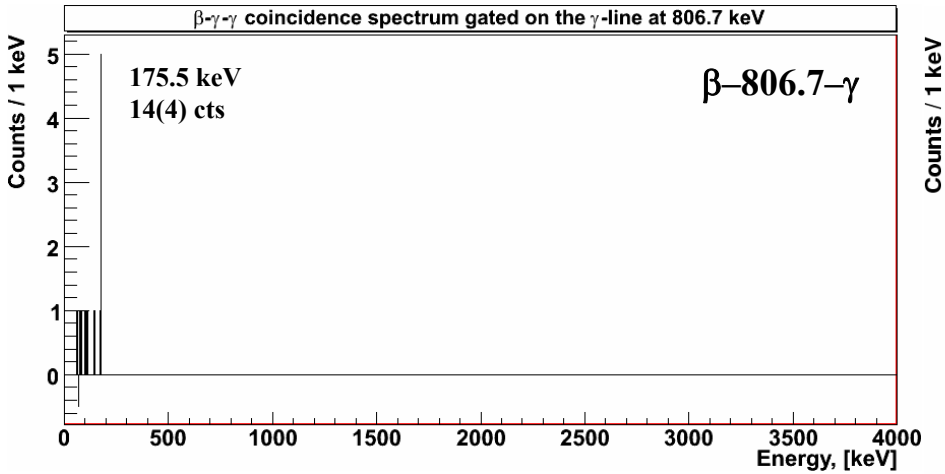

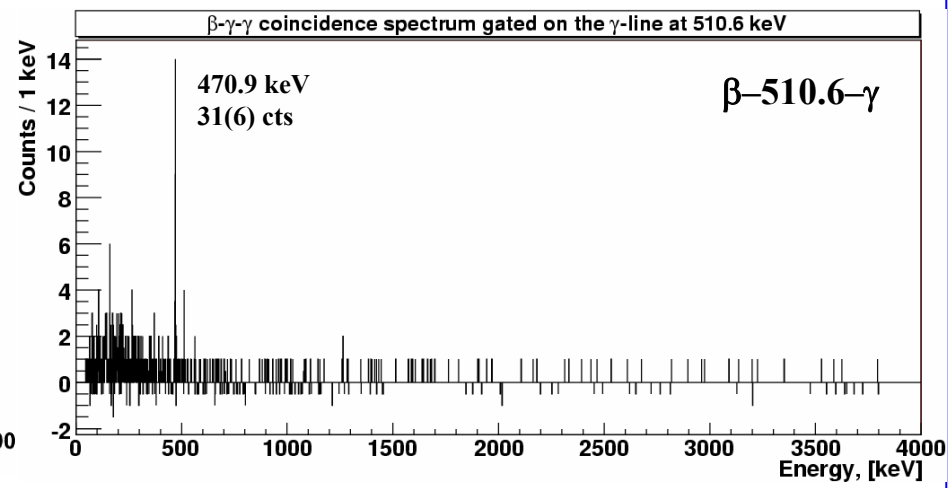

175.5 & 806.7 keV transitions are in cascade, 806.7 keV is on top of 175.5 keV

510.6 & 470.9 keV transitions are in cascade, their ordering cannot be determined

Other transitions do not yield coincidences

Discussion – Nuclear structure of ^{66}Co: the level scheme

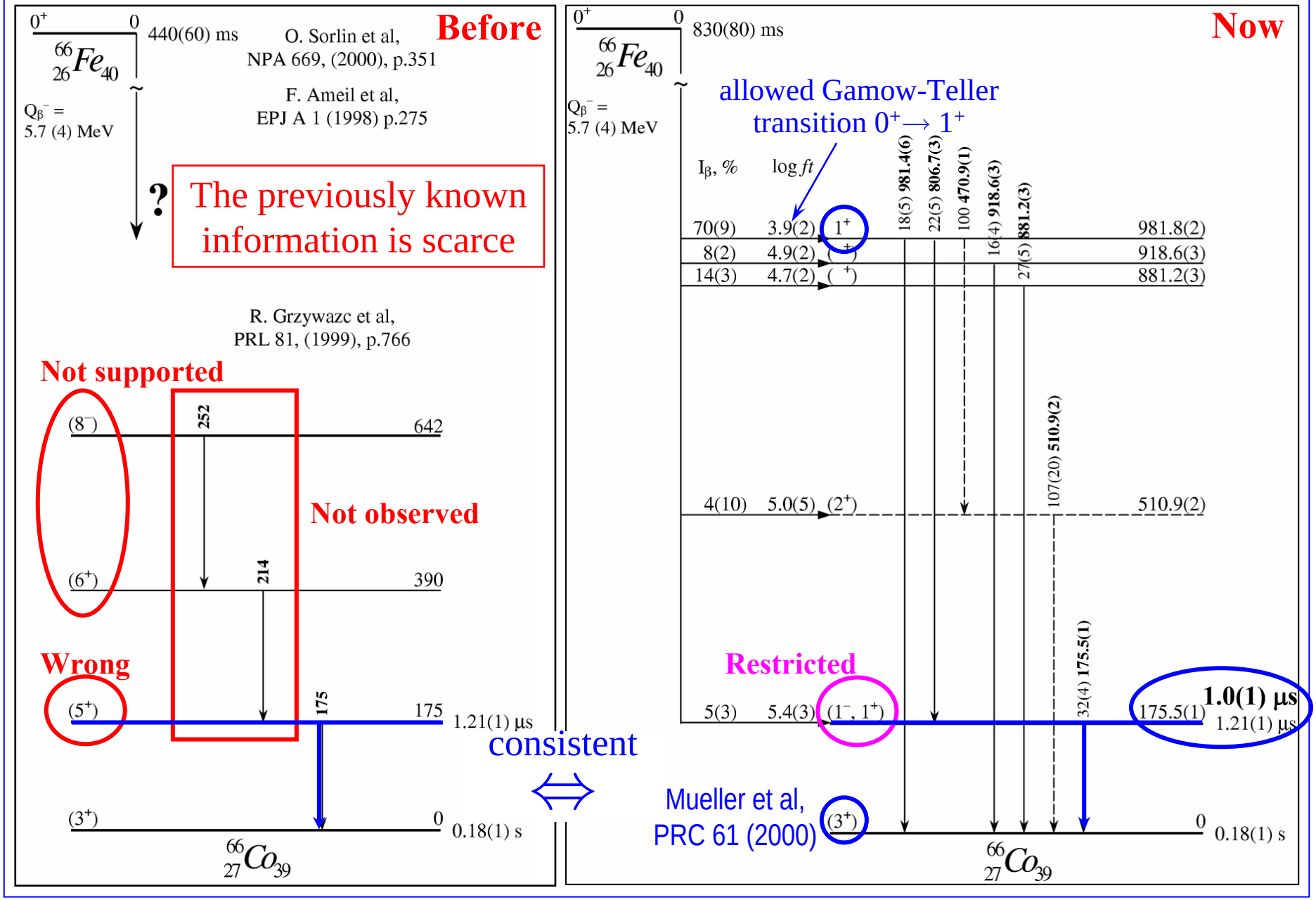

Discussion – Nuclear structure of ^{66}Co: interpretation

Paar's rule: Paar, NPA 331 (1979)
Spin multiplets
from the π–ν residual interaction

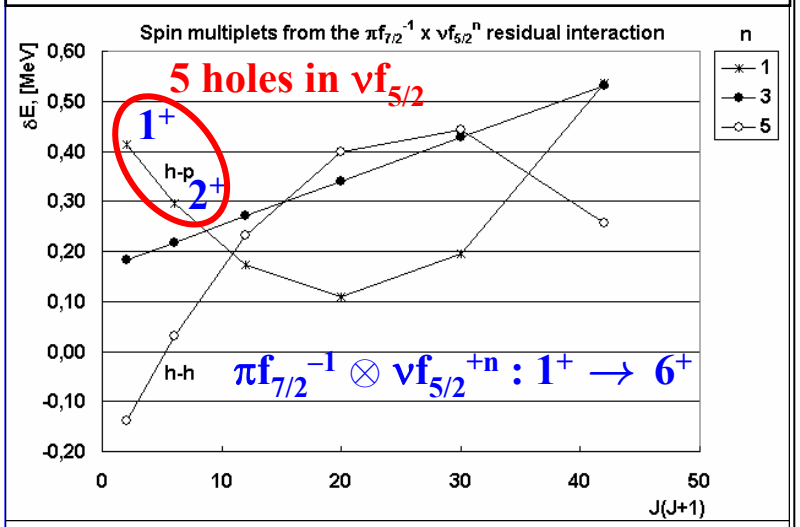

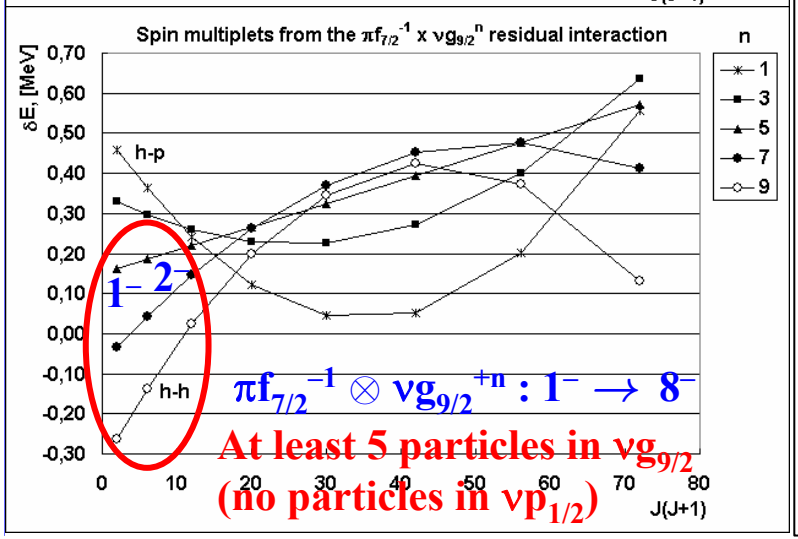

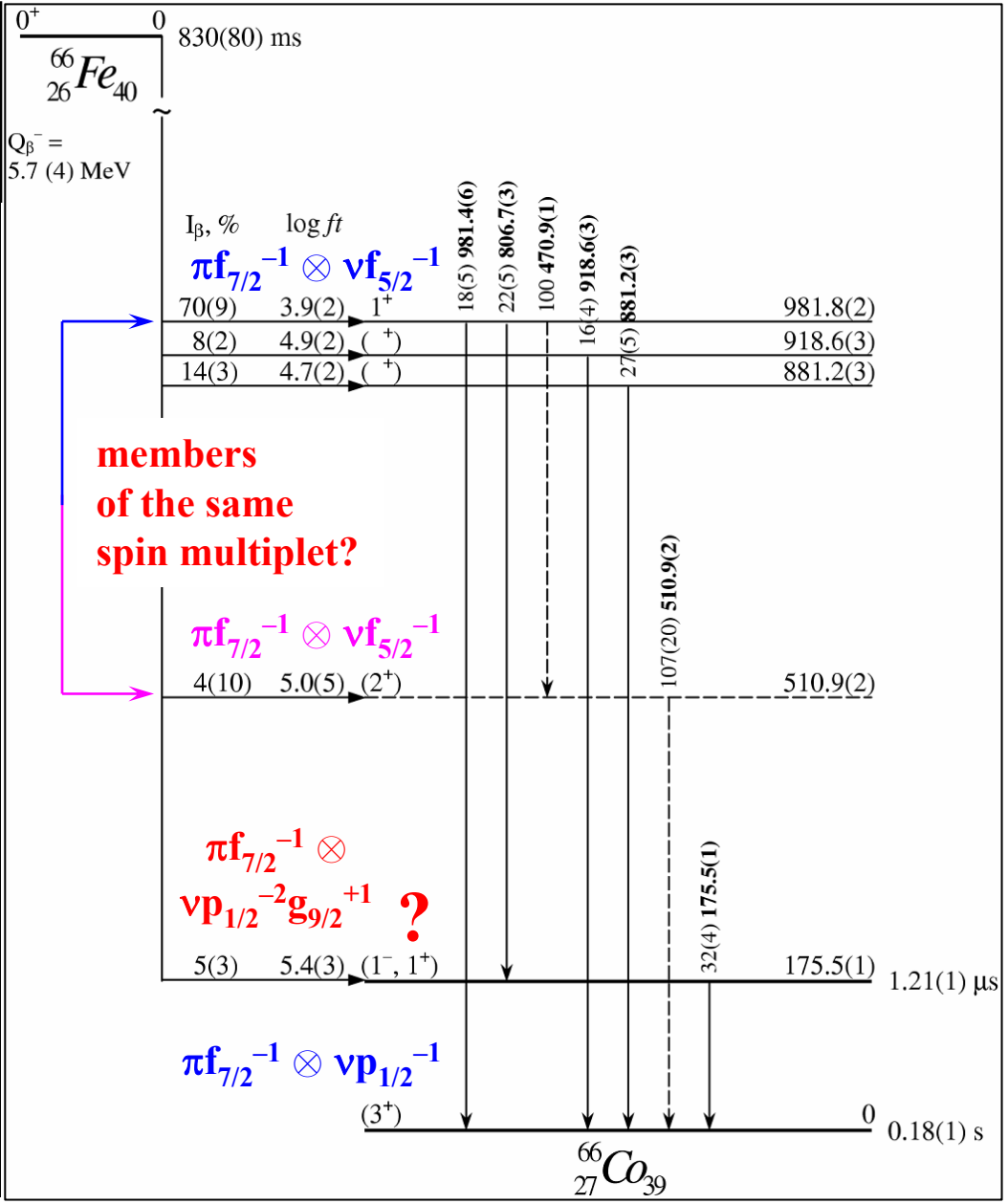

Data-acquisition System

Single detector

Spectroscopy Amplifier

Analogue-to-Digital Converter

Energy

Timing Filter Amplifier

Constant Fraction Discriminator

Time

Detector

DAQ PC

New data-analysis code based on C++ and CERN Root package was written to analyze new data

Segmented detector

x 4

Digital Gamma Finder DGF 4C

Crate Controller

Energy

Time

4 Channels

In order to acquire 21 / 39 channels
from one 6 / 12-fold segmented MINIBALL triple cluster detector
a new digital data-acquisition system had to be introduced

Performance of the β–γ-detection set-up as a low count-rate system

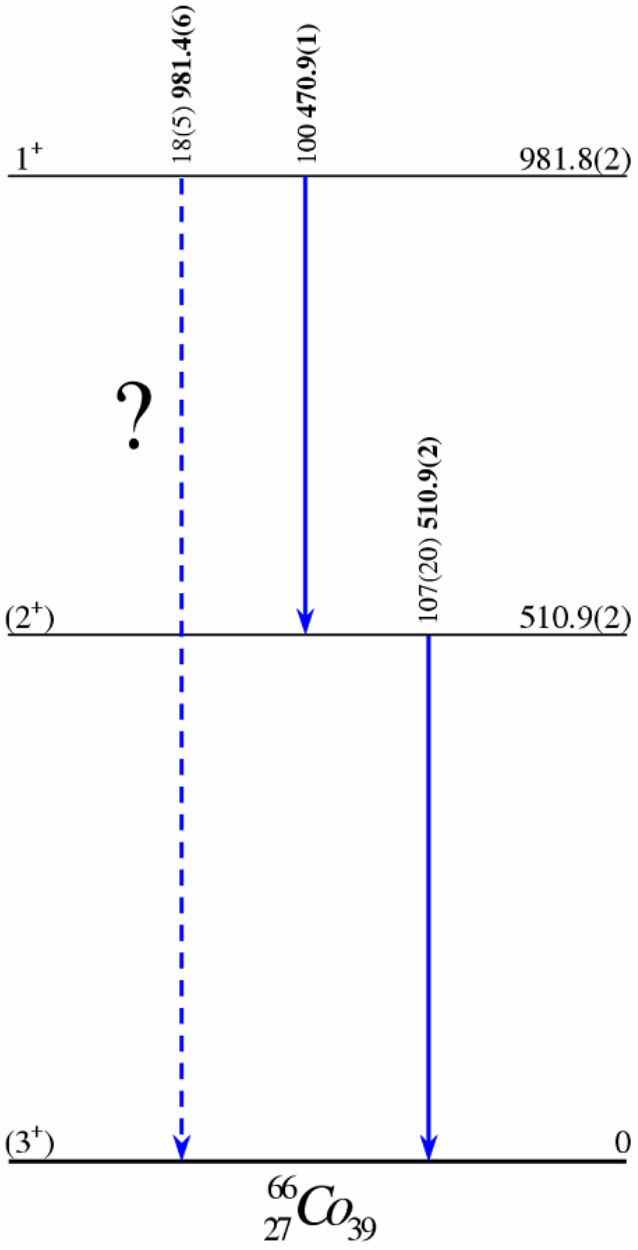

✓ γ-detection efficiency increased by ~1.5

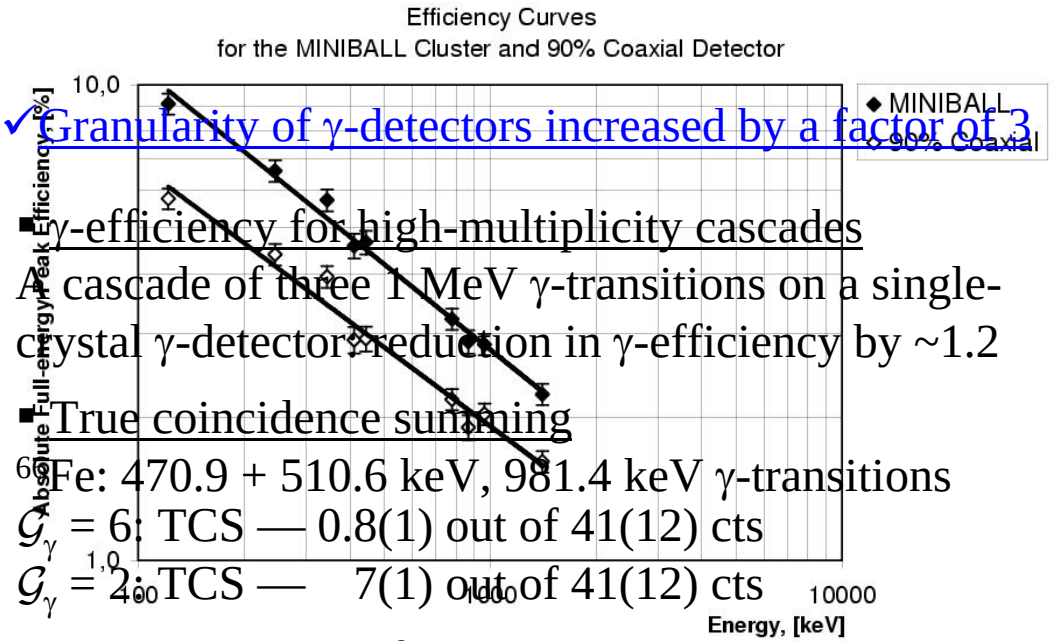

✓ Granularity of γ-detectors increased by a factor of 3

- γ-efficiency for high-multiplicity cascades

A cascade of three 1 MeV γ-transitions on a single-crystal γ-detector: reduction in γ-efficiency by ~1.2

- True coincidence summing

^{66}Fe: 470.9 + 510.6 keV, 981.4 keV γ-transitions

$\mathcal{G}_\gamma$ = 6: TCS — 0.8(1) out of 41(12) cts

$\mathcal{G}_\gamma$ = 2: TCS — 7(1) out of 41(12) cts

- Better selectivity for γ–γ-coincidences

✓ New multi-layer detector shielding installed

- Attenuation of the neutron flux increased by a factor of 2 / 5 for thermal / fast neutrons

Nuclear Structure along the Z=28 proton shell closure

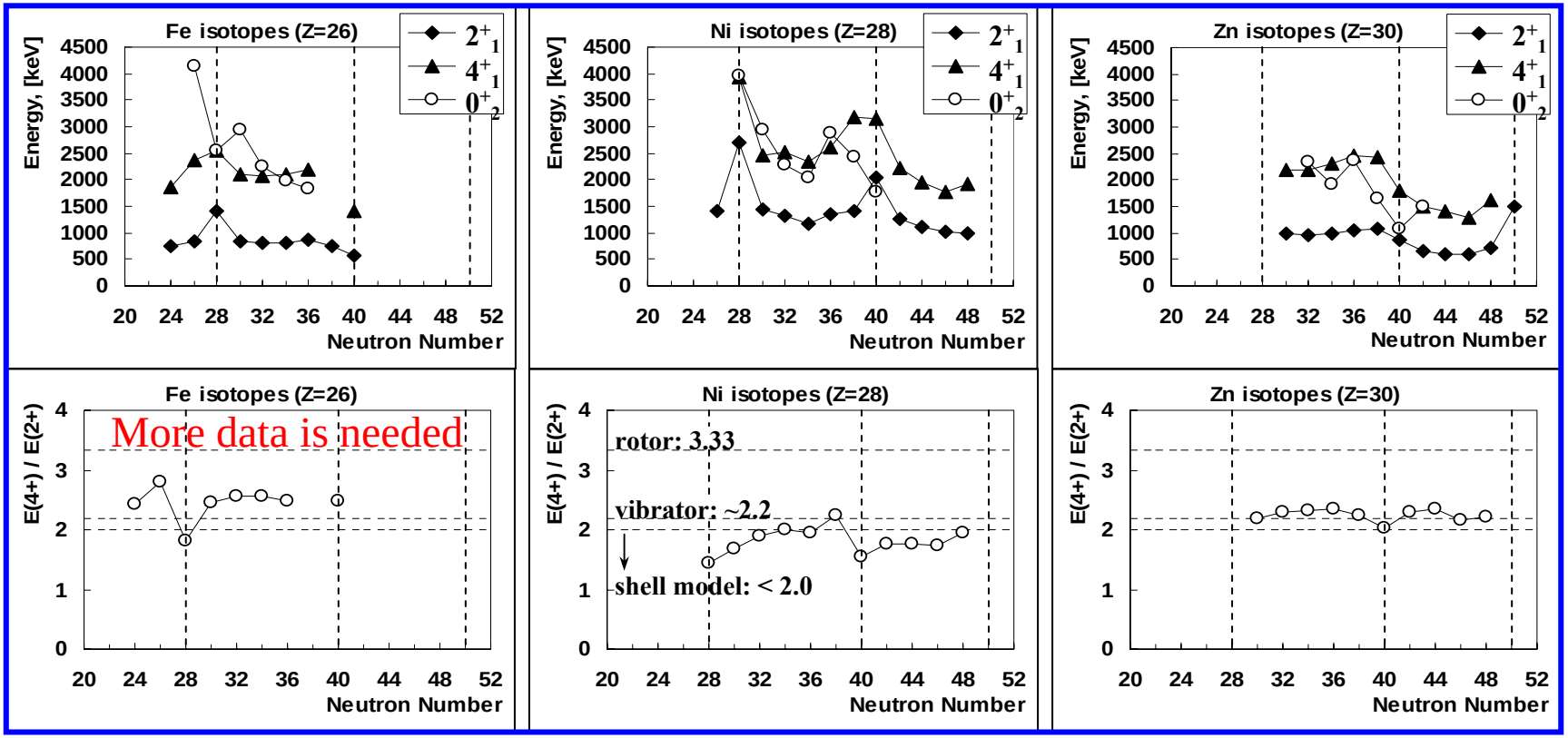

The Z=28 proton shell closure strongly influences the nuclear structure of Ni (Z=28) and neighboring Zn (Z=30) nuclei

However it is already weaker in neighboring Fe (Z=26) nuclei

A sustainable presence of this shell is expected in Co (Z=27) nuclei

The N=40 neutron subshell closure is not persistent in Zn and Fe nuclei

Results – β-decay of ^{66}Fe: half-life values

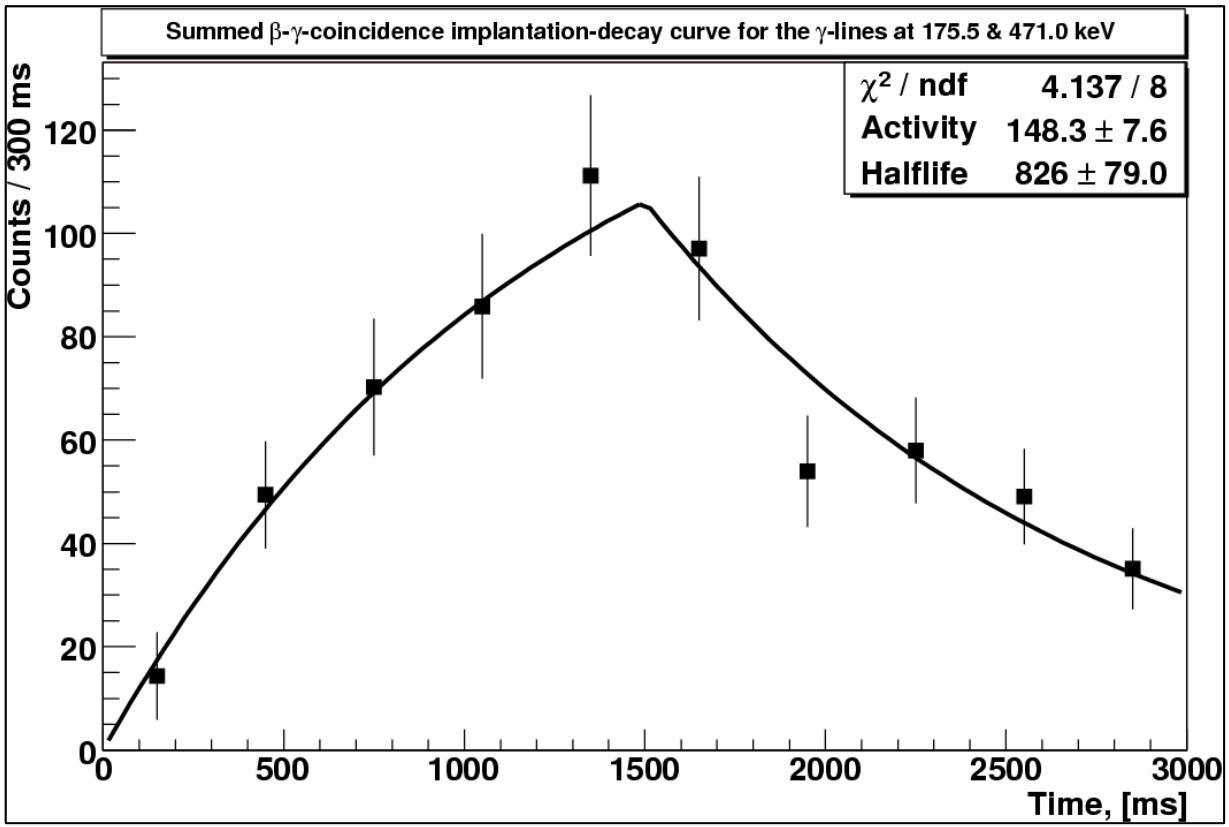

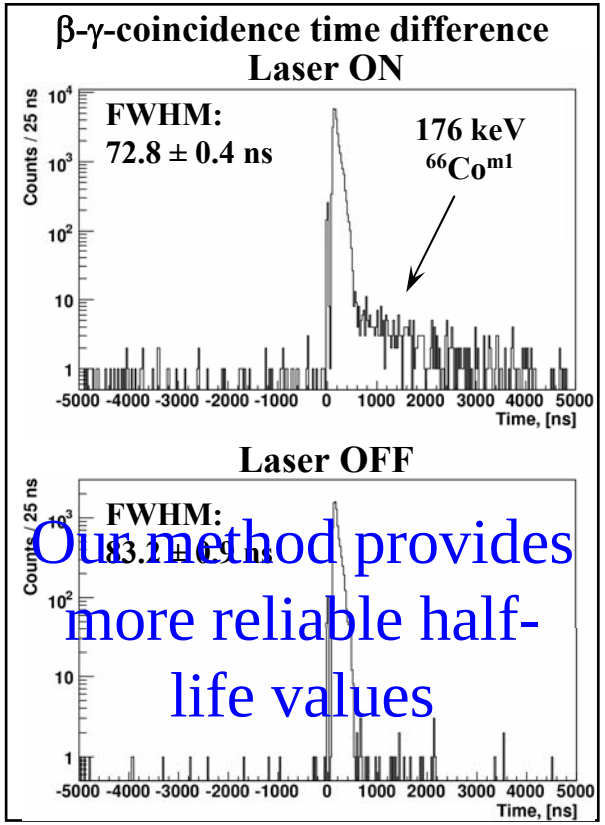

Our method provides more reliable half-life values

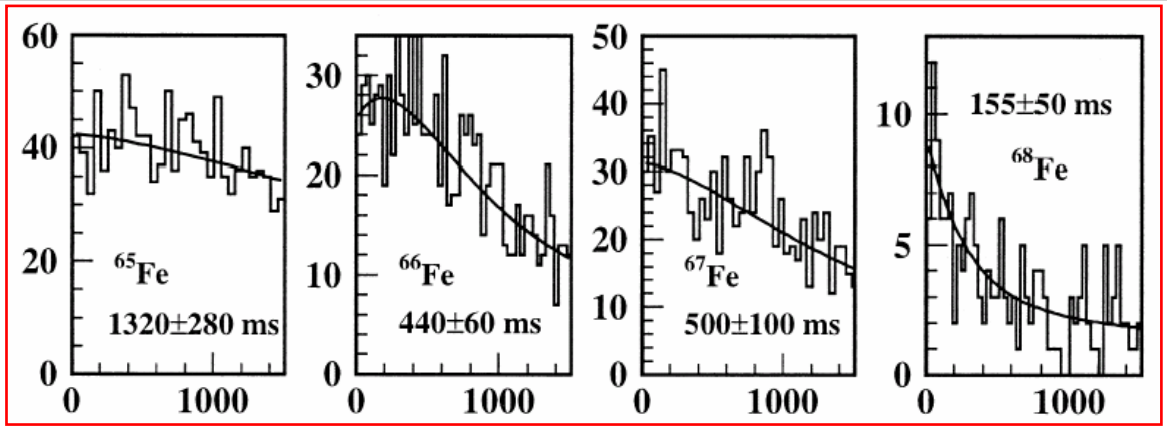

Extracted from time behavior of single β-particles

Sorlin *et al*, NPA 669 (2000)

Results – β-decay of ^{66}Fe

Fe isotope	^{63}Fe	^{64}Fe	^{65}Fe	^{66}Fe	^{67}Fe	^{68}Fe
$T_{1/2}$(Fe)	6.1 s	2.0 s	0.45 s	0.44 s	0.47 s	0.1 s
$T_{1/2}$(Co)	27.5 s	0.3 s	1.14 s	0.18 s	0.43 s	0.2 s
$T_{1/2}$(Ni)	100 y	stable	2.52 h	54.6 h	21 s	29 s
Production rate, [at/μC]	3.3	6.0	6.6	4.3	1.7	0.4
Number of known γ-lines	46	9	—	3	1	10
Decay scheme	Yes	Yes	No	No	No	No
Ground state β-feeding	80%	95%	?	?	?	?
Feasibility / Objective	No	No	Yes	Yes	Yes	No

Decay Properties: the case of ^{66}Fe

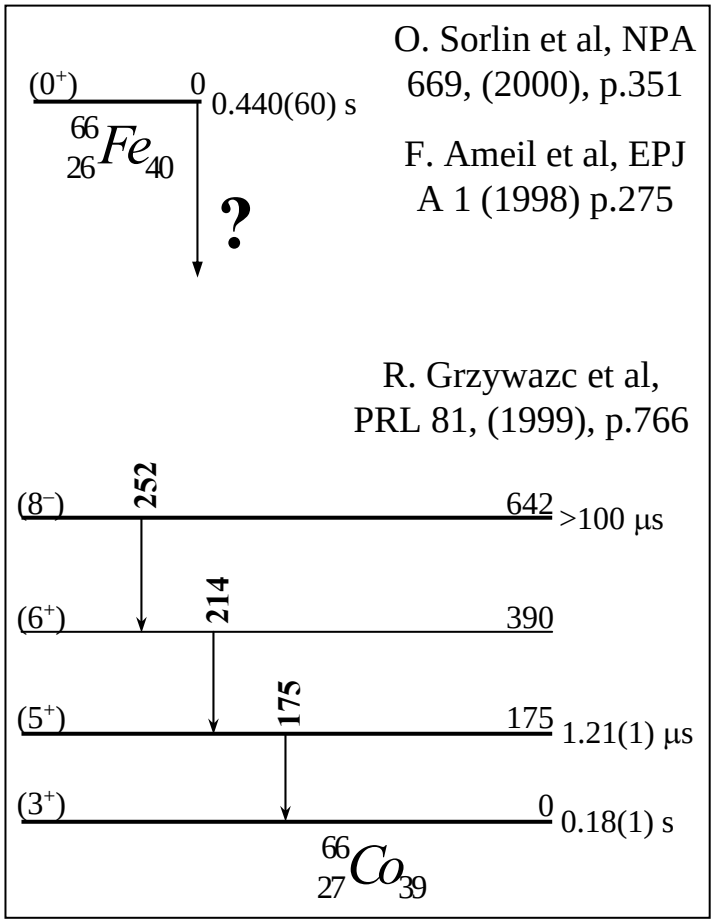

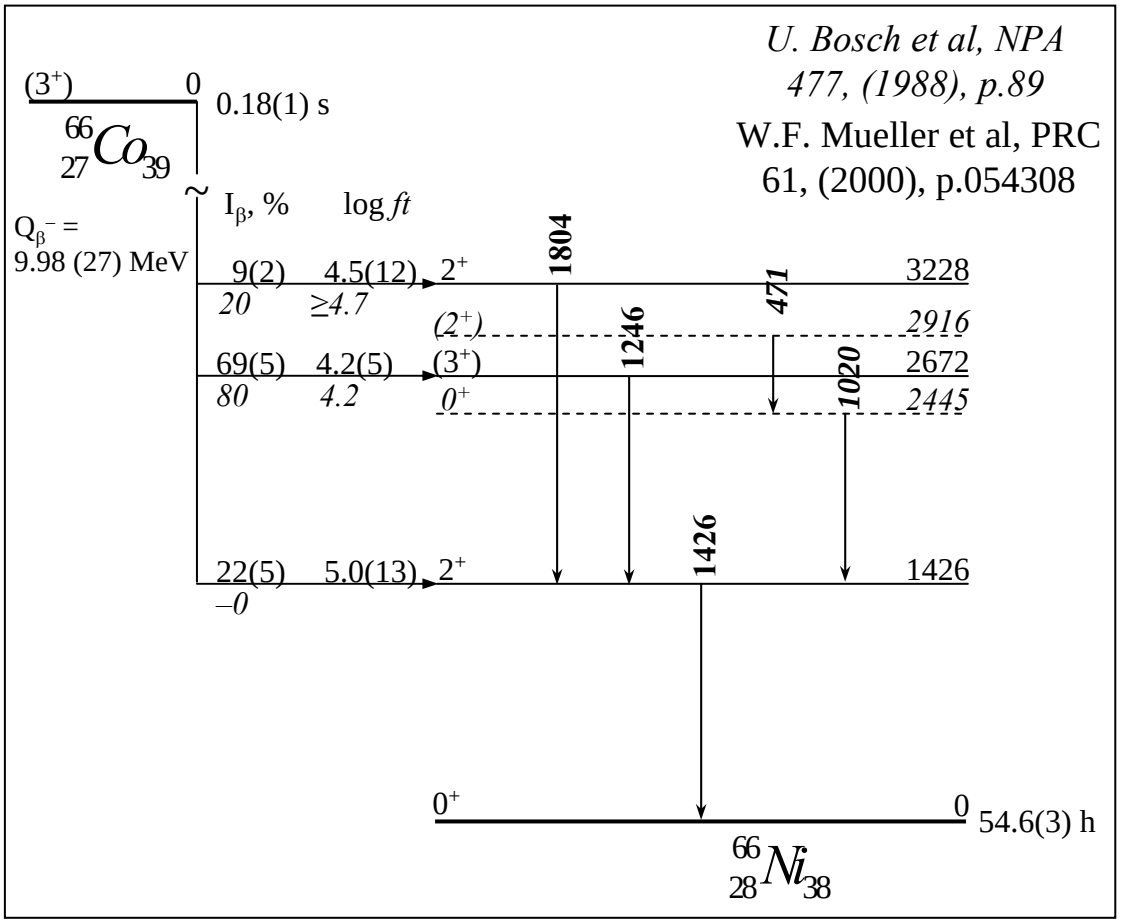

Fe, Co, Ni are refractory-type elements ⇒
Most studies were done using In-Flight separation method

No β-decay studies were performed for ^{66}Fe

Nuclear structure of ^{66}Co remains largely unknown

Data-acquisition System

Leading-edge timing (^{67}Fe, Nov. 2005)

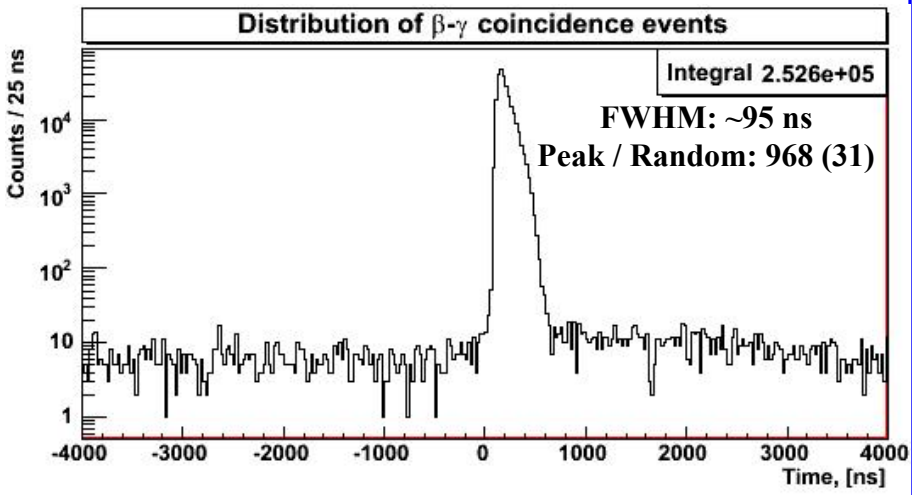

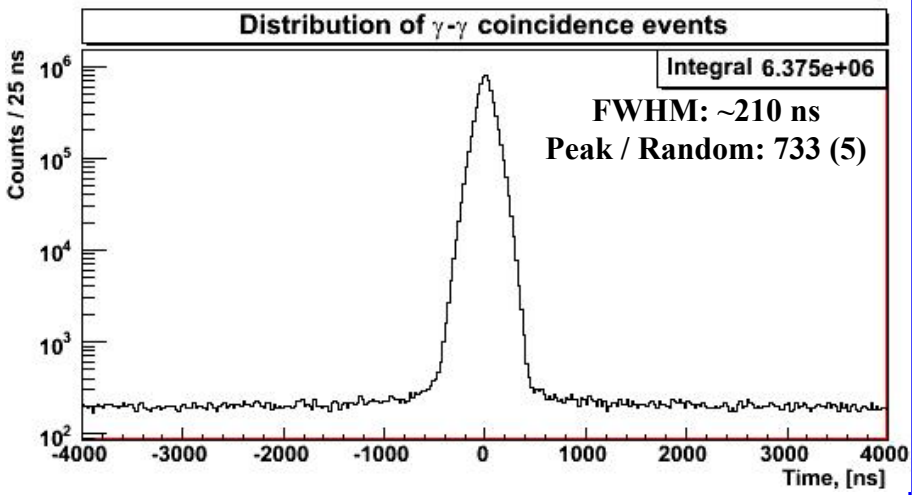

Constant-fraction timing (^{65}Fe, Jul. 2007)

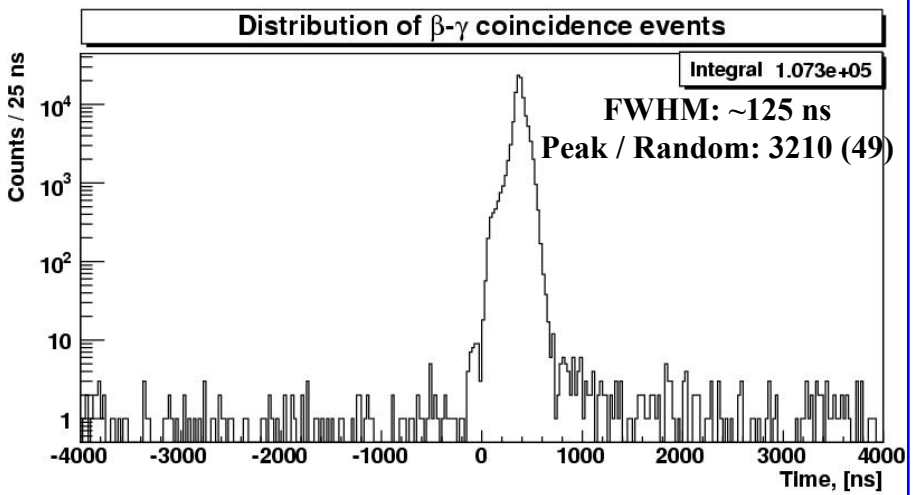

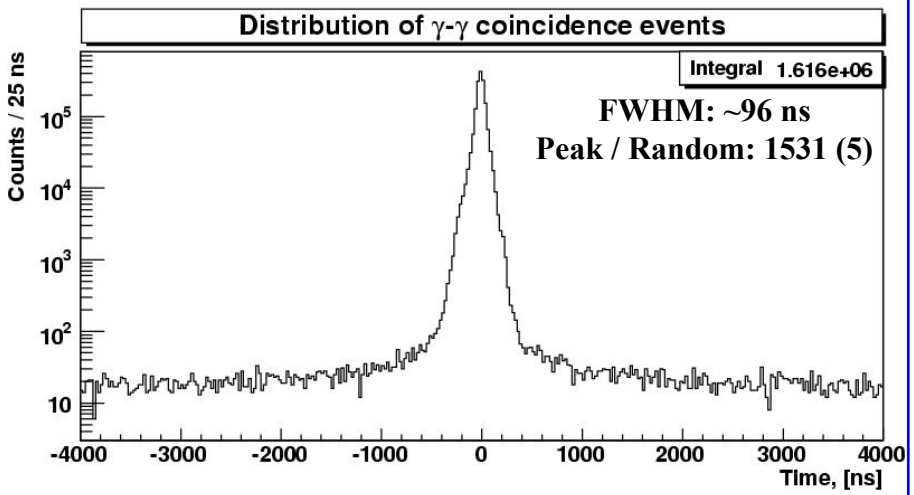

Implementation of the constant-fraction algorithm
improved the timing resolution by more than a factor of two

Results – β-decay of ^{66}Fe: Single γ-spectra

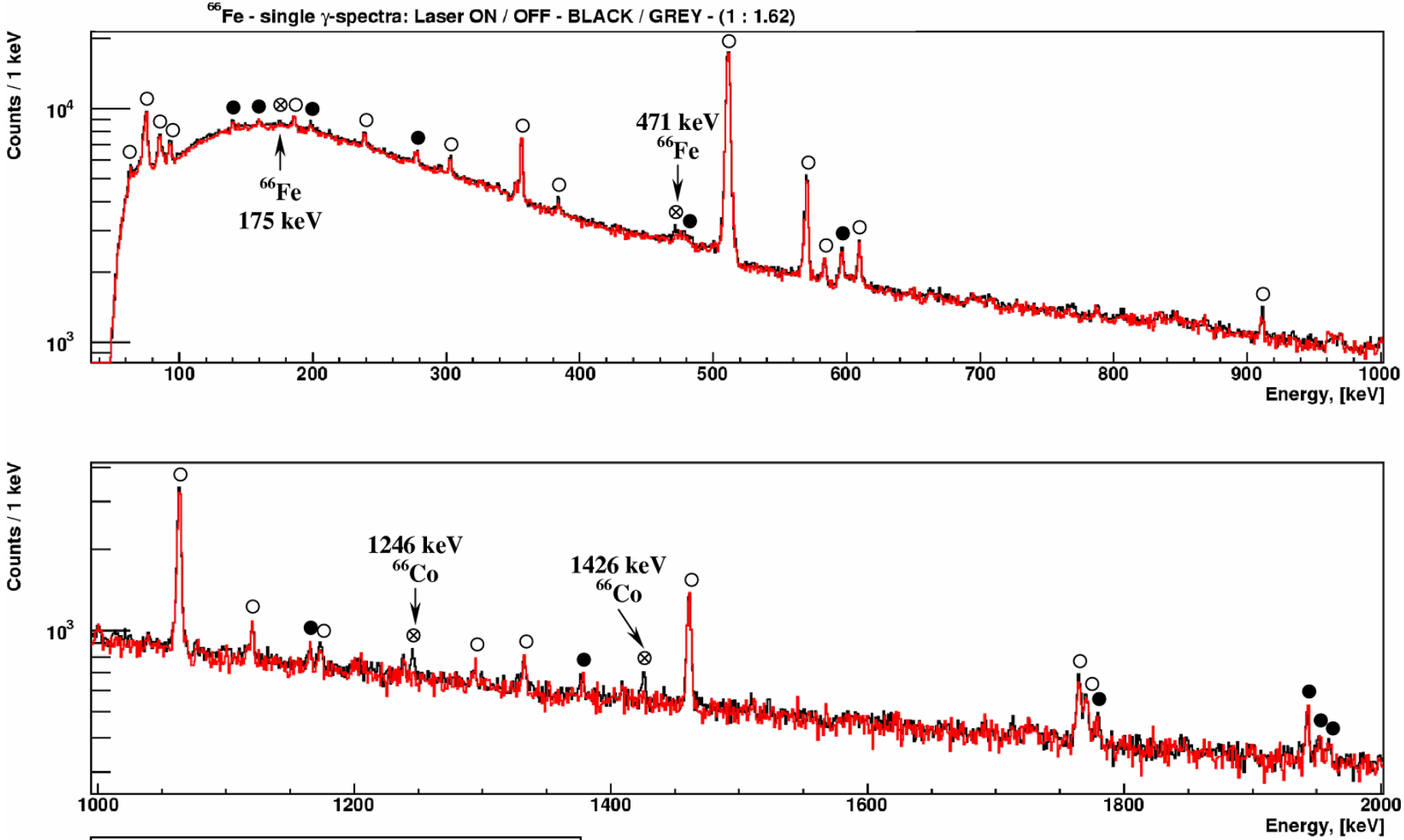

Discussion – Nuclear structure of ^{66}Co: the level scheme

1). ^{66}Fe: even-even nucleus
⇒ 0^+ ground state

2). ^{66}Co: (3^+) ground state based on dedicated studies at LISOL – Mueller et al, PRC 61 (2000)

3). 175.5 keV transition: *E2* / *M2*
⇒ $1^{+/-}$ or $5^{+/-}$ for the 175.5 keV level

4). 981.4 keV level: log*ft*=3.9(2)
⇒ allowed Gamow-Teller transition $0^+ \rightarrow 1^+$

5). 981.4 keV transition: multipolarity *E2*

6). 806.7 keV transition: *M1, E2* / *E1, M2*
⇒ $1^{+/-}$ for the 175.5 keV level

7). 175.5 keV level:
806.7 keV *M1* is much faster than 981.4 keV *E2*
⇒ not 1^+
806.7 keV *E1* is much faster than 981.4 keV *E2*
⇒ not 1^- ?
- *E1* can be strongly retarded — up to ~10^6
- no direct β-feeding

⇒ 1^- assignment

8). 470.9 & 510.9 keV level: multipolarity *M1*
⇒ (2^+) assignment for the 510.9 keV level

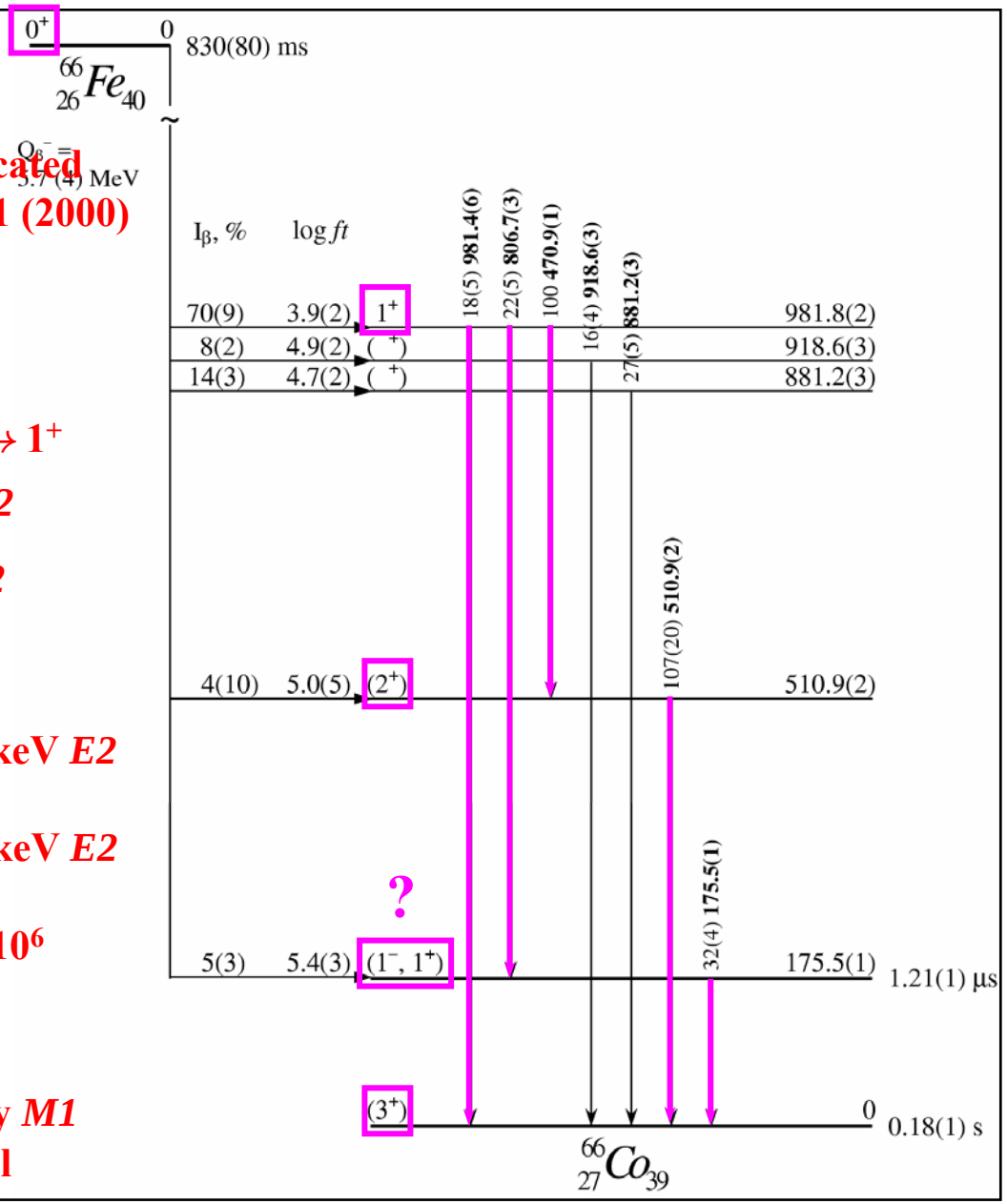

4-Channel Digital Gamma Finder

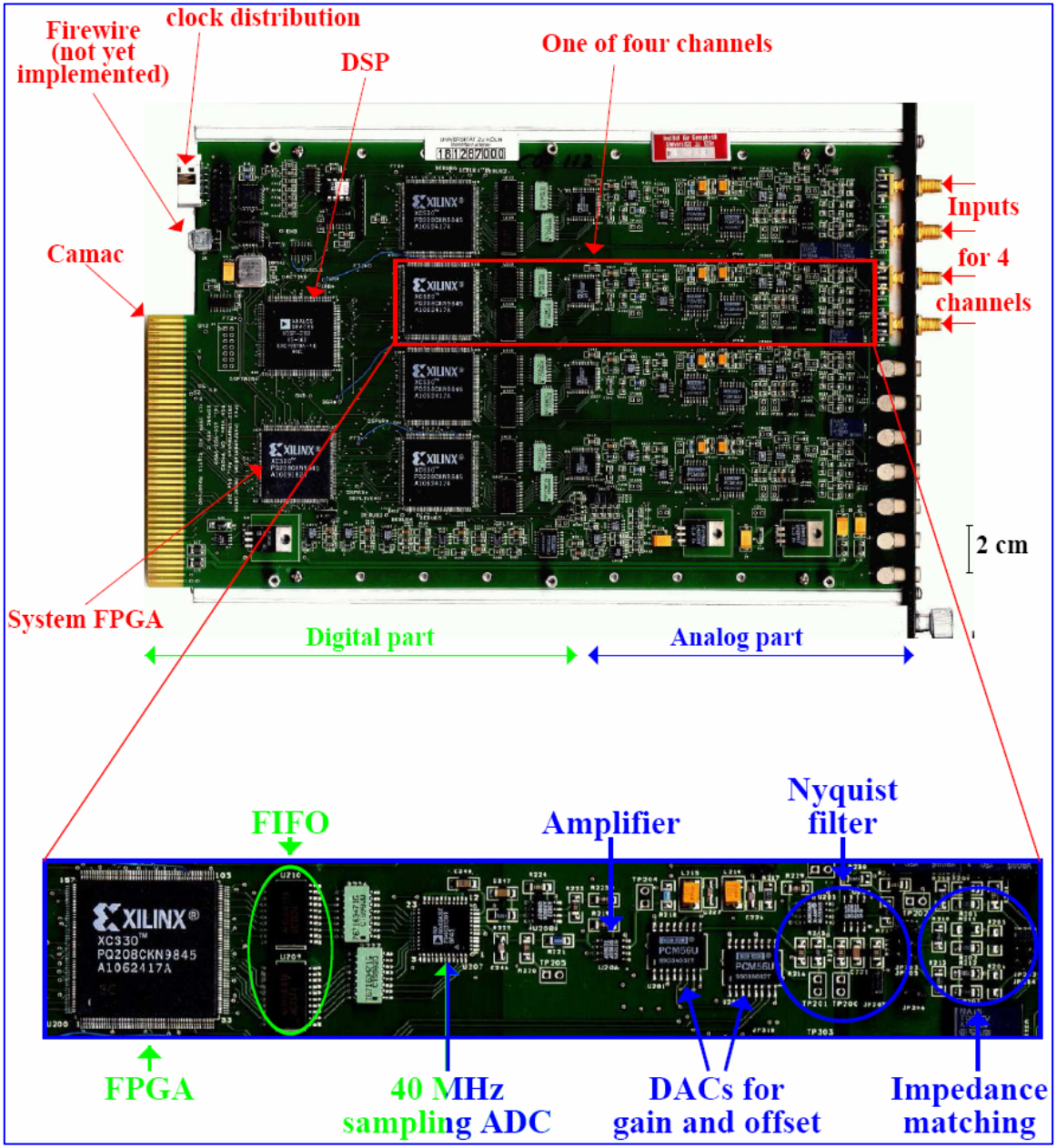

- **Analogue signal conditioning:** *adaptation of the incoming signal offset and gain to the ADC range.*
- **Real time processing:** *the FIFO memory is continuously filled with the waveform data from the ADC; with the FPGA the fast and slow trapezoidal filters are applied to detect the arrival of the signal and its pulse height; pile-up inspector issues a final trigger and interrupt request.*
- **Digital signal processor:** *programs the ASCU and RTPU hardware on initialization; reads raw data from all 4 RTPU's and stores it in memory; reconstructs pulse heights and applies time stamps from the 40 MHz clock; prepares the data for the output to the host computer.*
- **CAMAC interface:** *the host computer communicates with the DGFs and reads the data buffers.*

Results – β-decay of ^{66}Fe: β-gated γ-spectra

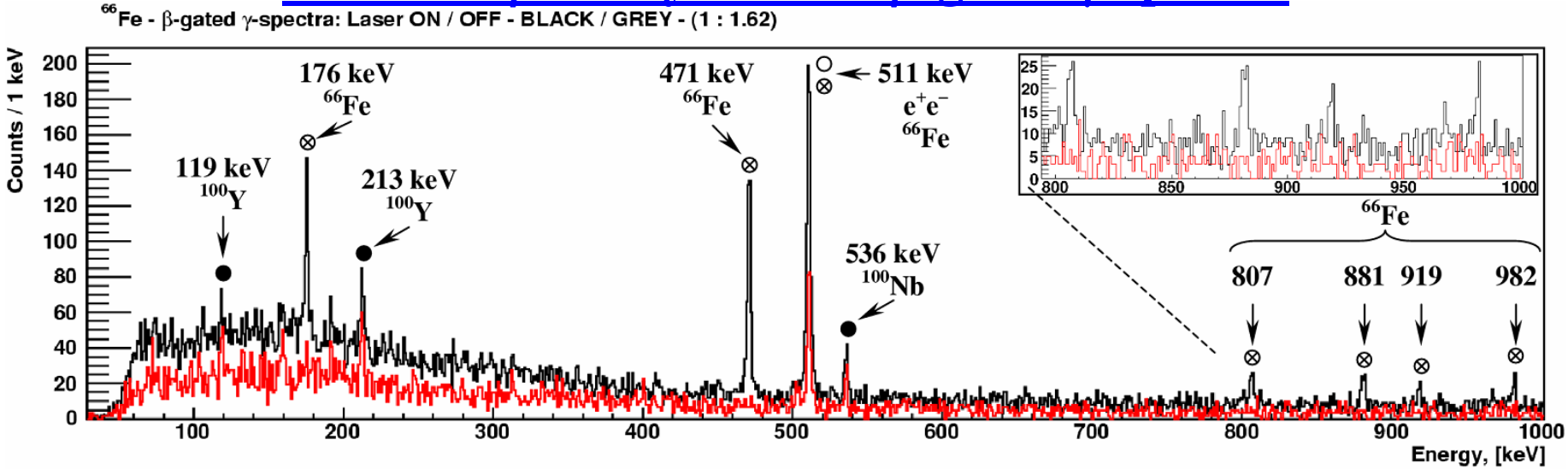

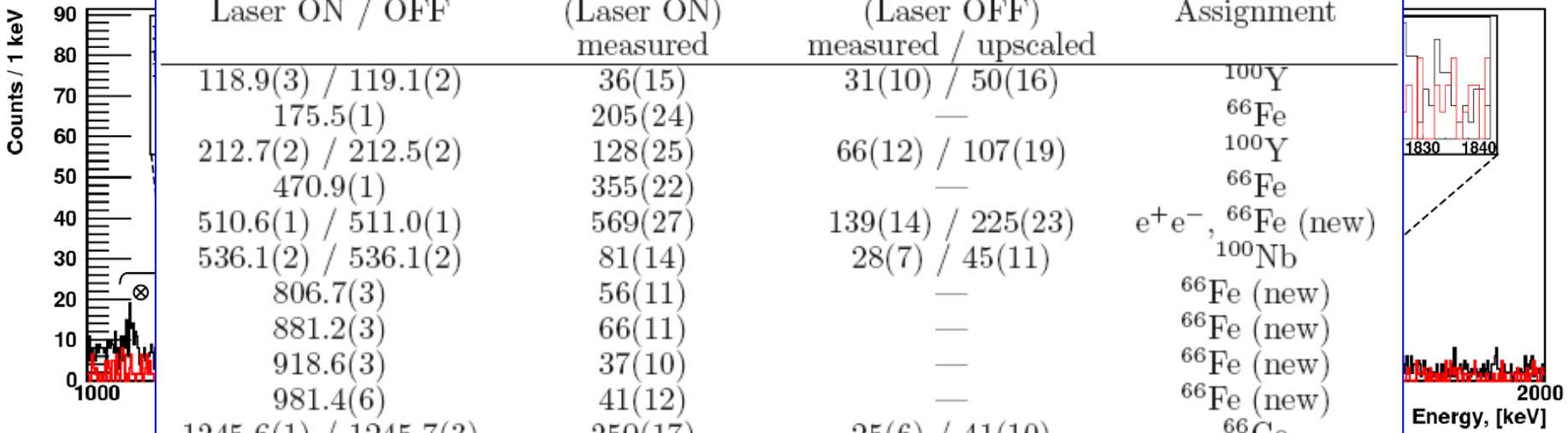

γ-line energy, [keV] Laser ON / OFF	Number of counts (Laser ON) measured	Number of counts (Laser OFF) measured / upscaled	Assignment
118.9(3) / 119.1(2)	36(15)	31(10) / 50(16)	^{100}Y
175.5(1)	205(24)	—	^{66}Fe
212.7(2) / 212.5(2)	128(25)	66(12) / 107(19)	^{100}Y
470.9(1)	355(22)	—	^{66}Fe
510.6(1) / 511.0(1)	569(27)	139(14) / 225(23)	e^+e^-, ^{66}Fe (new)
536.1(2) / 536.1(2)	81(14)	28(7) / 45(11)	^{100}Nb
806.7(3)	56(11)	—	^{66}Fe (new)
881.2(3)	66(11)	—	^{66}Fe (new)
918.6(3)	37(10)	—	^{66}Fe (new)
981.4(6)	41(12)	—	^{66}Fe (new)
1245.6(1) / 1245.7(3)	250(17)	25(6) / 41(10)	^{66}Co
1425.1(1) / 1425.1(4)	294(18)	30(7) / 49(11)	^{66}Co
1804.0(1.2)	33(10)	—	^{66}Co

Results – β-decay of ^{66}Fe: half-life values

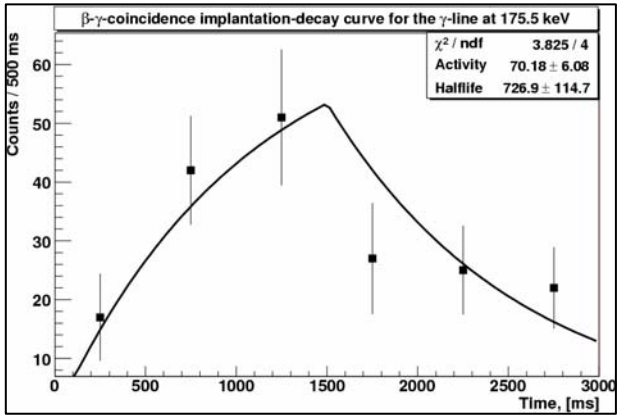

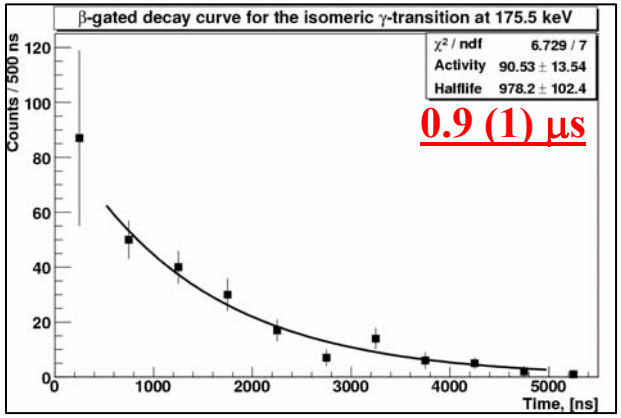

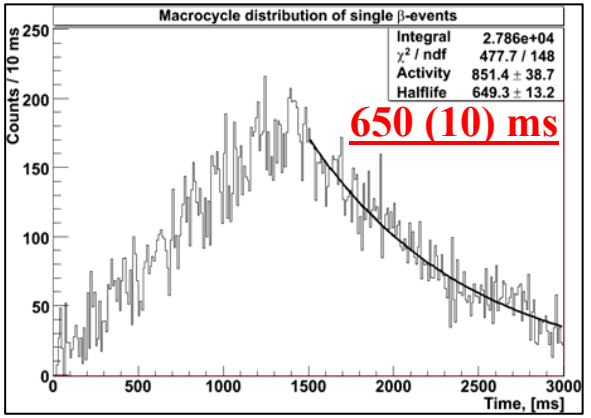

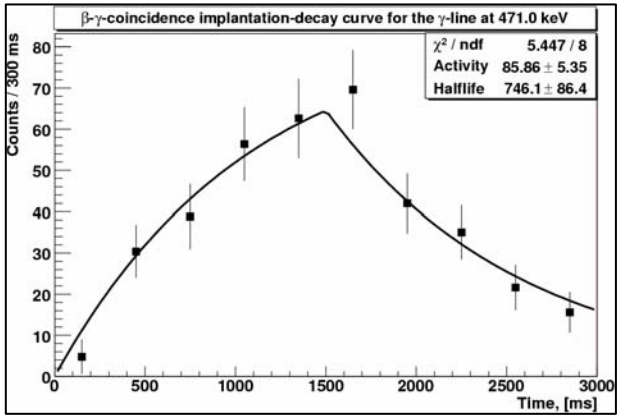

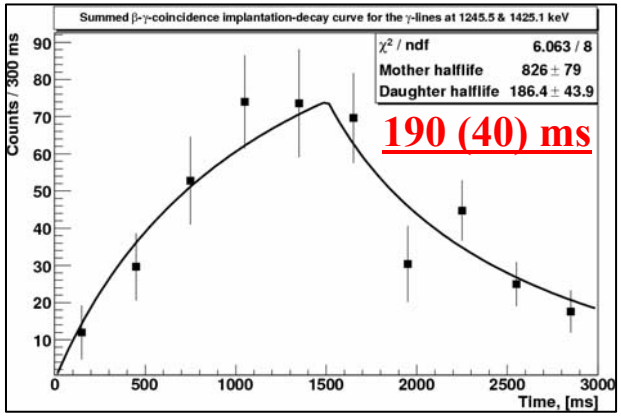

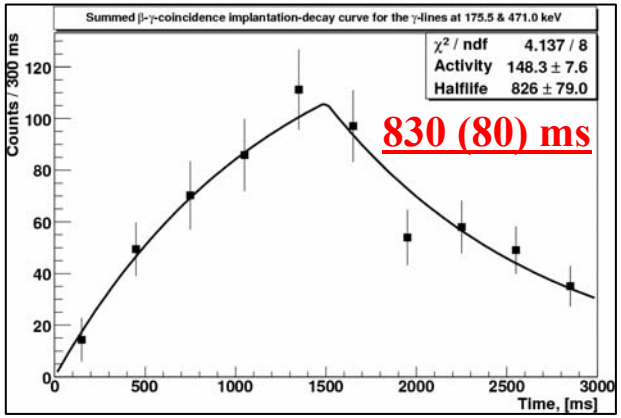

Sum of the β-gated statistics
from the γ-lines at 1246 & 1425 keV

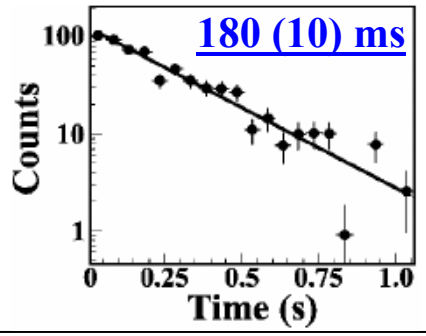

■ ^{66}Fe

Leuven: 830 (80) ms

literature: 440 (60) ms

Sorlin *et al*, NPA 669 (2000)

Ameil *et al*, EPJ A 1 (1998)

extracted from time behavior of single β-particles

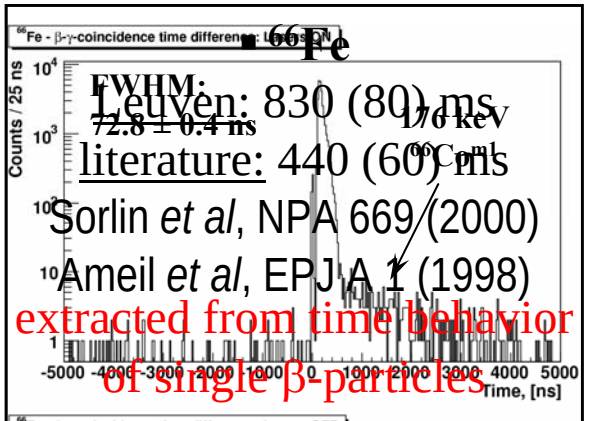

■ ^{66}Co

consistent with 180 (10) ms

Mueller *et al*, PRC 61 (2000)

■ ^{66m}Co

Leuven: 0.9 (1) µs

literature: 1.21 (1) µs

Grzywacz *et al*, PRL 81 (1999)